



Predicting river mouth location from delta front dip and clinoform dip in modern and ancient wave-dominated deltas

EVA H. ZIMMER  and JOHN A. HOWELL 

Department for Geology and Geophysics, University of Aberdeen, Meston Building, Meston Walk, Aberdeen AB24 3UE, UK (E-mail: john.howell@abdn.ac.uk)

Associate Editor – Christopher Fielding

ABSTRACT

Wave-dominated deltas and strandplains make up the majority of the world's depositional coastlines, provide an important record of sea-level change and serve as hydrocarbon reservoirs worldwide. Satellite imagery forms a great source of data on the recent depositional history of modern deltaic systems. In the subsurface, three-dimensional seismic and well data make the three-dimensional assessment of large-scale deltaic reservoir bodies possible but struggle to resolve internal heterogeneities away from wells. To bridge this gap in characterizing deltaic sedimentation, this study combines measurements from both the shallow, high-resolution section of three-dimensional seismic data of the Eocene Halibut Delta in the Outer Moray Firth, offshore Scotland, with information from Google Earth's satellite imagery and digital elevation model on south-east Brazilian river deltas (São Francisco, Jequitinhonha, Doce and Paraíba do Sul) to present a means of predicting the location of fluvial sediment input points with respect to clinoform geometry. The key measurement for this study is the delta front and clinoform dip which has been measured at multiple locations along strike of the coastline of the examined deltas. Dip decreases away from the inferred river mouth for all deltas by 50% within 7.2 km. The river mouth location was inferred from the position of palaeo-channels visible on the delta top and coarse sediment recorded in grab samples offshore for the south-east Brazilian deltas, and from imprints of palaeo-channels on attribute maps for the Eocene Halibut Delta. In summary, this study found that delta front dip is steepest at the location of the river mouth and decreases, along with grain size, away from it. This suggests that high dip values correlate with the proximity to the channel mouth and can be used to predict fluvial channel facies in modern deltaic systems and subsurface reservoirs.

Keywords Clinoform, clinoform dip, clinotherm, coastal processes, delta front, facies distribution, river-dominated, wave-dominated.

INTRODUCTION

Wave-dominated deltas and strandplains comprise 62% of the world's depositional coastlines (Nyberg & Howell, 2016). They provide an important record of sea-level change in the recent past (Dominguez *et al.*, 1987; Bhat-tacharya & Giosan, 2003; Anthony, 2015) and they serve as arable living space for a large

part of the world's population (Small & Nicholls, 2003; Nicholls *et al.*, 2007). Such systems are also important hydrocarbon reservoirs in the subsurface (Kantorowicz *et al.*, 1987; Løseth & Ryseth, 2003; Howell *et al.*, 2008; Hampson *et al.*, 2015). The modern and geologically recent depositional systems provide valuable data for analogue studies to understand the facies distribution and the

depositional history of these more deeply buried intervals.

Characterization of modern delta front systems starts with maps and bathymetric data. It is augmented with near-surface geophysical data such as ground-penetrating radar (Rocha *et al.*, 2013; Hein *et al.*, 2013) or shallow seismic data (Schwamborn *et al.*, 2002). These studies are costly to carry out and the number of acquired lines is often quite low. The recent availability of free global remote sensing data and elevation data made available through Google Earth© in 2005 has added considerably to current study of modern depositional systems (Hartley *et al.*, 2010; Nyberg & Howell, 2016; Evenstar *et al.*, 2018; Hartley *et al.*, 2018; Santos *et al.*, 2019).

In the subsurface, data availability has progressively improved over the last 40 years. Two-dimensional seismic lines available in the 1960s and 1970s provided the first insight lines, typically spaced a kilometre apart (Cartwright & Huuse, 2005). The advent of three-dimensional seismic data in the 1980s and 1990s made it possible to view features in the subsurface in 3D with tens of metres to metres accuracy (Cartwright & Huuse, 2005). Three-dimensional seismic data undergoes continued improvement with typical bin spacings of 12.5 m and long offsets providing very high-resolution data. These surveys are typically aimed at imaging reservoir depths and the upper portion of the data is largely ignored. However, the shallow, high frequency section of conventional 3D seismic data is an often-overlooked resource that offers high resolution insights into sedimentary and stratigraphic architecture.

This paper combines data from modern systems with data from the shallow portion of conventional seismic to examine wave-dominated deltas. Specifically, variability in clinoform dip angles along a series of wave-dominated delta fronts and their relationship to fluvial input points is analysed. Using data from both modern and ancient systems allows for combining the different strengths of these types of data. Satellite imagery and elevation data from the modern systems examined along the south-eastern coast of Brazil offer good control on the present-day facies distribution on the delta top, as well as some insight into the recent past. Within the modern systems, delta front dip is inferred from bathymetry and there is no insight into the internal architecture of the delta front deposits. Geometric data based on 3D seismic data from the Eocene Halibut Delta in the Outer Moray Firth

of the North Sea Basin (Zimmer *et al.*, 2019) provides information on the delta front development through time, although imaging the facies distribution on the delta top in these systems can be problematic. Combining both types of data enables the relationship between clinoform dip development in multiple sections along strike, the location of fluvial input points, and the facies distribution on the delta top to be uncovered. This relationship can inform reservoir modelling as well as sampling of modern systems to investigate their recent past.

CLINOFORMS

Clinofolds are basinward dipping surfaces which record the palaeo-depositional surface. They occur at a variety of discrete scales from the very large (continental margin scale) to the much smaller systems that are characteristic of shallow-marine deltaic and shelf-edge deposits which are the focus of the current study (Rich, 1951; Johannessen & Steel, 2005; Patruno *et al.*, 2015a). Clinoforms are packages of sediment bound above and below by a clinoform (Rich, 1951). The stacking pattern of clinoforms as well as the onlap, top lap and down lap that define their terminations have been studied along 2D seismic lines applying the concept of seismic stratigraphy ever since the technique's advent in the 1970s (Vail *et al.*, 1977). The height and dip of clinoforms has been used as a means of distinguishing between the different scales with deltaic systems typically tens of metres high and dipping at <15°, and shelf edge clinoforms typically hundreds of metres high with clinoform dips <6° (Johannessen & Steel, 2005; Patruno *et al.*, 2015a). An offspring of seismic stratigraphy and the usage of 2D seismic cross-sections is the development of the shoreline trajectory concept by which the upper rollover point of successive clinoforms is connected by a trajectory (Helland-Hansen & Martinsen, 1996). The shoreline trajectory represents the migration path of a shoreline or shelf edge and can be used in its most simple form to classify whether the system is regressive (migrating seaward) or transgressive (migrating landward) (Helland-Hansen & Martinsen, 1996; Henriksen *et al.*, 2009; Henriksen *et al.*, 2011). The concept has been extended to give information on sediment accumulation as well as sea-level change (Helland-Hansen & Hampson, 2009), uncovering the depositional system of successive clinoforms

(wave-dominated or river-dominated) and their potential to deliver sediment offshore (Henriksen *et al.*, 2009; Cosgrove *et al.*, 2018). The two datasets used in this study are presented in the following sections, starting with the modern, Brazilian study, and then compared and discussed.

SOUTH-EAST BRAZILIAN DELTAS – SÃO FRANCISCO, JEQUITINHONHA, DOCE AND PARAÍBA DO SUL

Study area

The south-eastern coast of Brazil between Recife in the north and Rio de Janeiro in the south is characterized by numerous wave-dominated deltas and shorefaces along a passive margin (Fig. 1). For this study, measurements of the delta front of four deltas along this stretch of coastline have been taken. The deltas were chosen due to their similarity with the Halibut Delta in terms of depositional process classification, grain-size distribution and delta plain area (especially São Francisco and Paraíba do Sul). Additionally, all of these deltas have been studied in the past, with data available on their offshore sediment deposits and dating of palaeochannels. From north to south the examined deltas are the São Francisco, Jequitinhonha, Doce and Paraíba do Sul river deltas. These four deltas are fine sand-dominated systems, with grain sizes ranging from fine to coarse sand, displaying a cusped shape characteristic for wave-dominated deltas (Orton & Reading, 1993). The tidal regime is microtidal to mesotidal (Table 1; Martin *et al.*, 1993; Dominguez, 1996; Oliveira *et al.*, 2012), with the tidal range increasing from south to north (Dominguez, 2009). The shelf width along the south-east Brazilian coast increases from 24 km in front of the São Francisco delta to 82 km in front of the Paraíba do Sul delta (Table 1). The south-east Brazilian coastline is situated within the Southern Hemisphere trade wind zone with prevalent winds coming from the north-east and south-east. The river plumes of the deltas studied here are affected by the orientation of the coast, the direction of the prevailing winds, and the resulting Ekman transport (Oliveira *et al.*, 2012). The river plumes of the north-east/south-west oriented São Francisco and Doce deltas are perpendicular to the coast whereas the river plumes of the north-south oriented Jequitinhonha and

Paraíba do Sul deltas are deflected towards a more coast-parallel direction (Oliveira *et al.*, 2012). Longshore sediment transport influences the symmetry of wave-dominated deltas and their sediment and facies distribution. Stronger longshore drift will enhance delta asymmetry and additionally deflect the river mouth down-drift (Bhattacharya & Giosan, 2003). Sediments deposited updrift are usually more mature through higher wave influence, as opposed to the more riverine influenced sediments down-drift (Martin & Suguio, 1992; Bhattacharya & Giosan, 2003). The modern systems studied here are mostly of symmetrical plan view shape with only the Doce and Paraíba do Sul deltas exhibiting slight asymmetry (Bhattacharya & Giosan, 2003). However, a facies asymmetry through differences in the influence of waves and riverine sediment deposition is displayed by all four deltas. The São Francisco River forms the boundary between the states of Sergipe and Alagoas with the São Francisco Delta located roughly 320 km SSE of Recife. With 634 000 km² the São Francisco has a larger drainage basin than all other East Brazilian rivers combined (622 600 km², Table 1, Souza & Knoppers, 2011). The São Francisco River delivers sediment offshore to the Sergipe-Alagoas Basin. 320 km south of Salvador, the Jequitinhonha River forms a delta in the state of Bahia and discharges into the Jequitinhonha Basin offshore. The Doce River flows through the state of Espírito Santo with its delta roughly 500 km ENE of Rio de Janeiro, prograding into the Espírito Santo Basin offshore. The delta plain of the Doce River covers an area larger than the other three delta plains combined (Table 1). The Paraíba do Sul delta is the southernmost delta examined in this study. It is situated 260 km ENE of Rio de Janeiro and discharges into the Campos Basin offshore.

Geological history and delta development

During the breakup of the supercontinent Gondwana in the Cretaceous, South America and Africa separated following lithospheric extension and rifting Chang *et al.*, 1992; Macdonald *et al.*, 2003; Mohriak *et al.*, 2008). Fully marine conditions were established at the transition from Lower to Upper Cretaceous (Albian–Cenomanian, Chang *et al.*, 1992; Mohriak *et al.*, 2008). While rifting along the Atlantic Mid-Ocean Ridge continues to this day, the influence of active rifting on the south-east Brazilian coastal basins investigated here ceased during



Fig. 1. Four modern deltas along the south-east Brazilian coast were analysed as part of the study. The studied deltas are marked by red squares and are shown in detail in Figs 3 to 6. This map shows their location, the extent of their drainage area and the associated offshore basin.

Table 1. Selected characteristics of the south-east Brazilian deltas. Delta plain area and shelf width in front of the river mouth were measured in Google Earth© as part of this study. The other data are derived from Oliveira *et al.* (2012), Souza & Knoppers (2011), Patchineelam & Smoak (1999) and Martin *et al.* (1993).

	Drainage basin area [km ²]	Annual mean river flow [m ³ s ⁻¹]	Delta plain area [km ²]	Shelf width at river mouth [km]	Tidal range	Prevailing wind direction
São Francisco	622 600	1800	847	24	Mesotidal	NE, SE
Jequitinhonha	67 769	434	368	27	Microtidal	ENE, SSE
Doce	75 800	900	2364	27	Microtidal	NE, SE
Paraíba do Sul	55 500	865	772	82	Microtidal	ENE, SSE

the Upper Cretaceous and subsequent subsidence was due to sediment loading and thermal relaxation rather than rifting (Chang *et al.*, 1992; Lawver *et al.*, 1992). In the offshore section of the south-east Brazilian basins, a succession of

fluvial, lacustrine and marine sediments, including a thick succession of evaporites, was deposited during the Late Jurassic to Cretaceous (Milani *et al.*, 2007). Onshore of the south-east Brazilian basins, Cenozoic sediments directly

overlie the Proterozoic and Cambrian Brazilian Shield. The Sergipe/Alagoas Basin is an exception to this where sediments from all rift phases, including Late Jurassic pre-rift deposits, are preserved in a narrow band along the coast (Darros de Matos, 1999). The most significant and widespread sedimentological unit underlying the Quaternary deltas is the Upper Miocene to Lower Pleistocene Barreiras Formation. The fine to coarse-grained sandstone and conglomerate deposits of the Barreiras Formation have been described as continental fluvial and alluvial deposits (Jequitinhonha Basin, Vilas Boas *et al.*, 2001) or as marginal marine, tidal deposits (Sergipe/Alagoas Basin, Rossetti & Góes, 2009). Through epeirogenetic uplift and continued erosion throughout the Quaternary, the Barreiras Formation forms cliffs along the south-east Brazilian coast (Rossetti & Góes, 2009). During the Upper Pleistocene sea-level highstand (123 ka, Andrade *et al.*, 2003), regressive wave-dominated deltas formed along the Brazilian south-east coast. These deltas were made up of 'regressive sandsheets' (Martin & Dominguez, 1994) and resembled the deltas developing at the present day, with beach ridges prograding basinward. This phase of regression lasted for most of the Upper Pleistocene until a transgression submerged the deltaic deposits from the end of the Upper Pleistocene (18 ka) onward into the Holocene (5.1 ka) (Andrade *et al.*, 2003). Lagoons and intralagoonal deltas developed during the 5.1 ka highstand (sea level 5 m higher than present day), submerging the Pleistocene prograding deltas and beach ridges (Martin & Dominguez, 1994). After this highstand, sea level dropped along the south-east Brazilian coast, causing the lagoons to develop into mangrove swamps. The subsequent deposition of regressive sandy beach ridges continues to the present day (Martin & Dominguez, 1994).

Methodology

The key measurement for this study is the dip angle of the delta front ('delta front dip') which is measured on the dip-parallel bathymetric profile of the delta front. The delta front dip is considered to be a proxy for clinof orm dip on the delta front and thus comparable to clinof orm dip measured in subsurface data. Delta front dip was measured at multiple locations along strike of the coastline of the studied deltas. To determine delta front dip, a path perpendicular to the present-day coastline is created in Google

Earth© and the elevation profile along this path is displayed (Data: SIO, NOAA, U.S. Navy, NGA, GEBCO). From the change in bathymetry between the upper and the lower rollover point and the distance between them, the delta front dip can be inferred (Fig. 2). Measurements derived from remote sensing data carry a horizontal and vertical error. The vertical resolution of Google Earth's bathymetric digital elevation model is dependent on the accuracy of the underlying depth data, the cell size, and the interpolation technique used (Weatherall *et al.*, 2015; Amante & Eakins, 2016). Because data for this study are measured in the coastal zone immediately adjacent to the coastline, it can be assumed that the depth data quality was high. South-east Brazil being close to the equator also means that data derived from satellite altimetry is of good quality due to the almost vertical path between satellite and measuring point (Weatherall *et al.*, 2015). In water depths below 200 m a data resolution below 1 m is possible (Mayer *et al.*, 2018). The horizontal resolution of satellite imagery data can be highly variable but is in this case assumed to be in an equal range to a recent study of the Doce River delta (between 0.5 m and 10 m, Polizel & Rossetti, 2014). Since the changes in distance and elevation measured here lie above 10 m and 1 m, respectively, horizontal and vertical accuracy is deemed sufficient to support the study's outcomes. To capture along strike variations in delta front dip, multiple measurements were taken along strike of the modern-day coastline of each of the examined deltas. Measurements were taken at an average spacing of 1.5 km along the coast for the São Francisco, Jequitinhonha and Paraíba do Sul rivers and at an average spacing of 2 km for the Doce River. This spacing was sufficiently small to identify changes in delta front dip and large enough to keep all datasets manageable and convenient to display. Clinof orm dip was measured along 32 transects for the Jequitinhonha delta front, along 38 transects for the Paraíba do Sul delta front, and along 44 transects for both the São Francisco and the Doce delta fronts.

Facies and sediment distribution on delta plain and delta front

Satellite imagery allows approximate interpretation of the delta plain sediments of all four analysed modern systems. This visual evaluation was augmented with published studies to gain a better understanding of the delta's evolution.

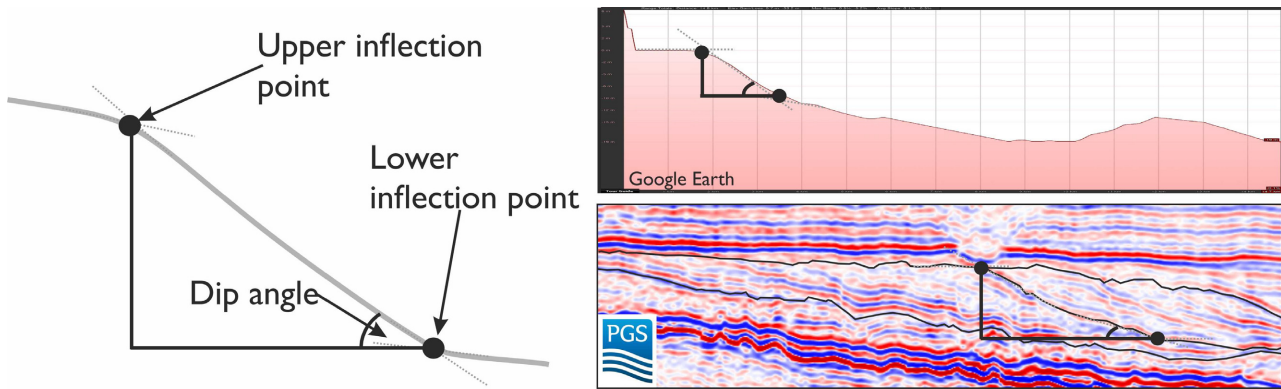


Fig. 2. Measurements of delta front dip and clinoform dip are taken on the slope between the upper and lower inflection point of the delta front/clinoform. Delta front dip is measured on a bathymetric profile and clinoform dip is measured on a seismic cross-section, both are oriented perpendicular to the (palaeo-) shoreline. This orientation has been observed to capture maximum dip in the data used but does not account for local variations such as spits.

Radiocarbon dating has been carried out on the Doce and Jequitinhonha delta plain (Dominguez *et al.*, 1987; Rossetti *et al.*, 2015) but is lacking for the São Francisco and Paraíba do Sul delta plains. The distribution of sediments at the delta front and further offshore has been deduced from sediment grab samples for the Doce and the Paraíba do Sul delta (Murillo *et al.*, 2009; Quaresma *et al.*, 2015) but is absent for the São Francisco and Jequitinhonha.

São Francisco

The active river channel of the São Francisco River has an S-shape on the delta plain and lies within a channel belt characterized by meander scrollbars. The channel sits in a central position within the delta (Fig. 3). The São Francisco River has been occupying this position for the last 5 ka (Dominguez, 1996). Longshore drift is directed towards the south-west and the beach ridges developed on the southern side of the channel are interspersed with more fine-grained riverine sediments than the beach ridges on the northern delta flank (Dominguez, 1996; Bittencourt *et al.*, 2005). Towards the north-east and south-west two canyons are visible, although the rivers occupying them are small and do not reach the sea at present. In the location of the northern canyon, the beach ridges are cut suggesting that there was a distributary (in the location of the current Piauí River) reaching the sea in the past just south of the headland of Pontal de Peba. Between Pontal de Peba and the river mouth of the São Francisco River, an aeolian

dune belt masks the most recent beach ridge development. A similar dune belt is active to the south of the delta although the dunes here show more vegetation. Palaeo-dune fields are visible further inland of both active dune fields.

Jequitinhonha

Similar to the São Francisco River, the active channel of the Jequitinhonha River and its channel belt occupy a central position on the Jequitinhonha delta plain (Fig. 4). However, longshore drift along the Jequitinhonha delta is directed towards the north (Bittencourt *et al.*, 2005). Beach ridges are visible in the north and in the south of the delta plain, but the beach ridges north of the Jequitinhonha River are disrupted by two meandering rivers (Pardo and Salsa rivers). Carbon-14 dating of the fluvial sediments deposited in the palaeo-channel belt yielded an age of 5.57 (± 0.15) ka (Dominguez *et al.*, 1987). It is thought that both of these northern rivers were active during most of the Holocene and contributed to beach ridge formation (Dominguez *et al.*, 1987; Martin *et al.*, 1993; Dominguez, 1996). The youngest beach ridge system has been dated to 2.57 (± 0.1) ka in its most landward position and the continuity of these beach ridges towards the north suggests that both northern rivers did not supply significant amounts of sediment to the delta from 2.5 ka to the present day (Dominguez *et al.*, 1987). South of the river the beach ridges are very uniform with only a few small channels in the far south of the delta.

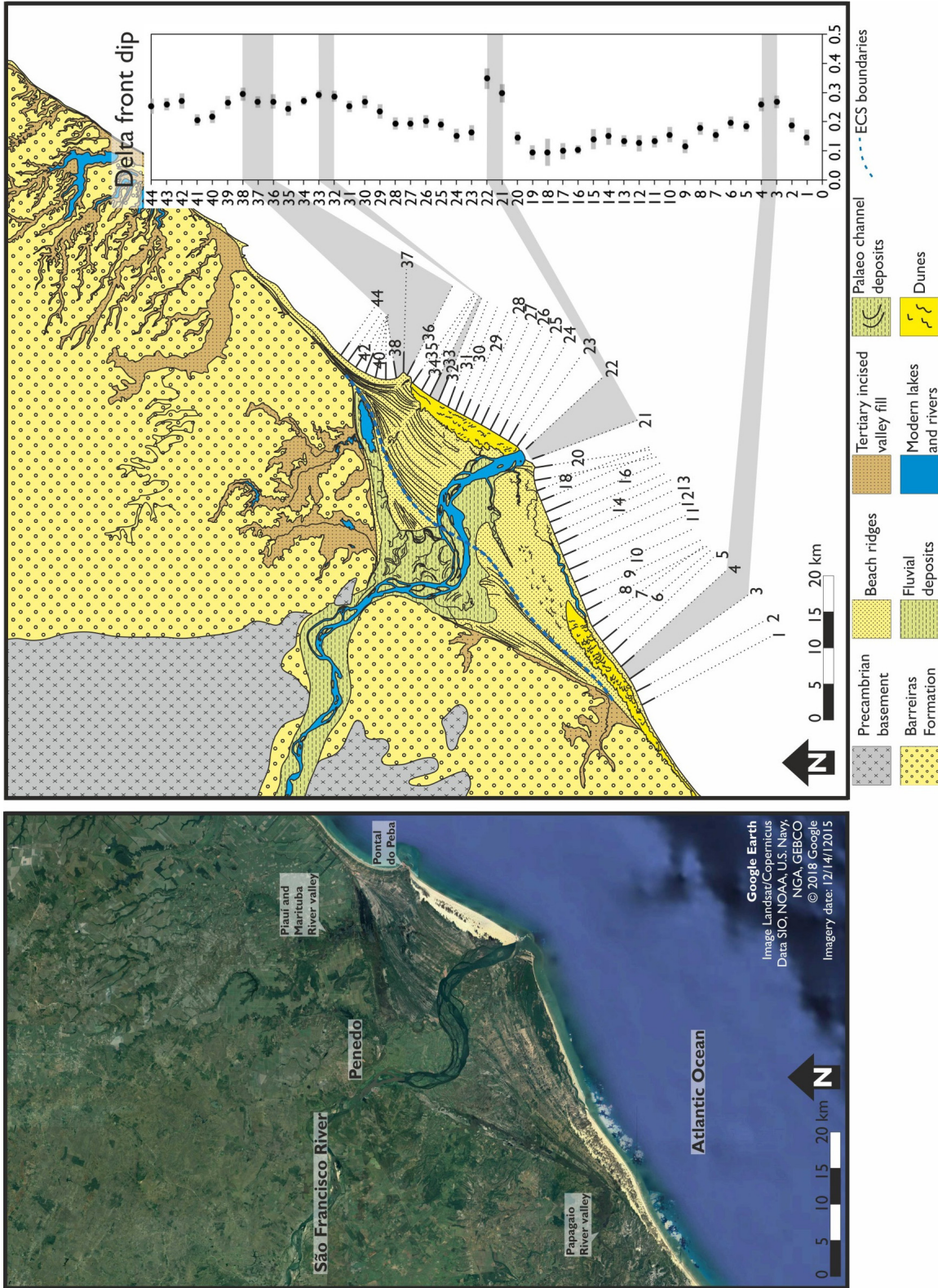


Fig. 3. Satellite view of the São Francisco delta (left) with interpreted facies distribution and clinof orm dip transects (right, error bars in grey are based on the inferred resolution of the remote sensing data). The placement of the element complex set (ECS) boundaries is based on Ainsworth *et al.* (2019). The extent of the Barreiras Formation is taken from Dominguez *et al.* (1987).

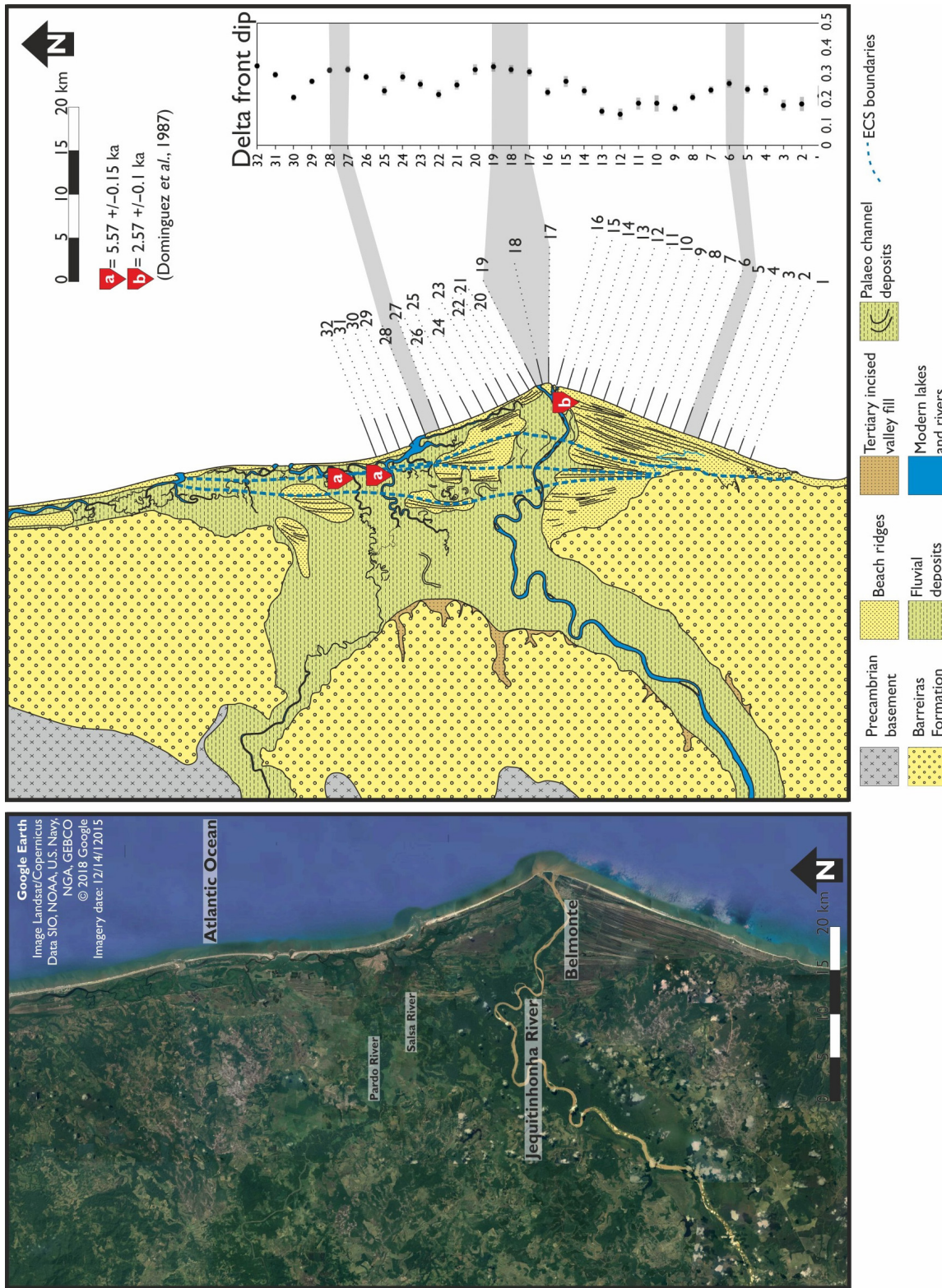


Fig. 4. Satellite view of the Jequitinhonha delta (left) with interpreted features and clinof orm dip transects (right, error bars in grey are based on the inferred resolution of the remote sensing data). The placement of the element complex set (ECS) boundaries is taken from Ainsworth *et al.* (2019). The extent of the Barreiras Formation is taken from Dominguez *et al.* (1987).

Doce

The Doce delta plain is characterized by at least four distinct palaeo-channels cross-cutting most of the delta plain (Fig. 5). Close to the escarpment enclosing the Doce River delta, the eroded remains of two older generations of beach ridges are visible. These beach ridges are truncated in a seaward direction by uniform deposits lacking distinct depositional features on satellite imagery but which have previously been characterized as interdistributary bay deposits (Rossetti *et al.*, 2015). Areas of tropical forest surround the palaeo-channels and the active river channel. The most recent advance of beach ridges is developed along the coast in a belt which is up to 10 km wide and thins significantly towards the north (<1 km). Longshore drift along the Doce delta is not uniform and may change direction during storm events (Quaresma *et al.*, 2015). A coast-parallel meandering river and associated lagoonal belt is developed in the north, immediately landward of the most recent beach ridge. Carbon-14 dating of the palaeo-channels yields ages of 10.8 (± 0.460) ka and 5.4 (± 0.401) ka for the southernmost channel visible on the delta plain and ages between 6.3 (± 0.541) ka and 5.7 (± 0.566) ka for the northernmost palaeo-channel (Rossetti *et al.*, 2015). The beach ridges visible on satellite imagery are either older (>7 ka, Cohen *et al.*, 2013) or younger than these palaeo-channels, although the most landward section of the youngest beach ridge belt is speculated to be associated with the northernmost palaeo-channel (Rossetti *et al.*, 2015). Sediment grab samples from the seabed at the delta front and offshore transition zone document coarse grain sizes (granules, coarse and medium sand) approximately 25 km north of the Doce River mouth in water depths between 10 m and 67 m (Quaresma *et al.*, 2015). Due to the additional high carbonate content and the high density of the deposits, this sediment has been classified as relict sands belonging to a past river mouth location (Quaresma *et al.*, 2015). Due to the high carbonate content, these sediments might be a remnant of Holocene lagoonal deposition. South of the river mouth, mud content is reported to be greater than 75% and is attributed to southward drift of a mud plume coming from the river mouth (Quaresma *et al.*, 2015).

Paraíba do Sul

The Paraíba do Sul River is situated in a northern-central position on the delta plain. Beach ridges are developed either side of the river in

continuous bands with the beach ridges south of the river crossed by several smaller streams (Fig. 6). The channel belt of the Paraíba do Sul River is relatively narrow measuring 6.5 km at its widest point. The northern edge of the delta plain is directly bordered by an escarpment cut by multiple incised canyons. In the south, the delta plain is not bounded by an escarpment but the beach ridges of the current delta pass landward (westward) into palaeo-channel deposits which are not clearly visible on satellite imagery due to the city of Campos and agricultural use of the land just south of the city. However, close to the southern coast, palaeo-meander bends are preserved and further west along the coast a second set of beach ridges unconnected to the current Paraíba do Sul delta plain is visible, with the Lake Feia lying inland of these beach ridges. During the Pleistocene, the Paraíba do Sul occupied an approximately 35 km long channel trending NNW–SSE from the present site of the city Campos towards the SSE facing coastline where it contributed to beach ridge formation (Martin *et al.*, 1985; Martin *et al.*, 1993). Longshore transport is not uniform along the Paraíba do Sul delta, with southward longshore drift around the river mouth and northward drift along the southern and northern delta flanks (Bastos & Silva, 2003). Sediment distribution in front of the current river mouth shows predominantly coarse sand within the first kilometre offshore, extending 4 km to the north and 2 km to the south of the river mouth along the coast (Murillo *et al.*, 2009). This coarse sand is followed by a 2 to 3 km wide mud belt in a seaward direction which stretches for at least 15 km north and southward (Murillo *et al.*, 2009). Four kilometres offshore from the current river mouth, very coarse and coarse sand is recorded at the delta front with a tongue of fine to medium sand extending *ca* 10 km in a coast-parallel direction from the river mouth to the south where the surficial sediment transitions to biogenic mud (boundary corresponding to transect 21 in this study, Murillo *et al.*, 2009).

Results on delta front dip at multiple sections along strike

Delta front dip along the south-east Brazilian deltas is not uniform but shows systematic variation. The São Francisco River has delta front dips of up to 0.32° towards the northern and the southern edge of the delta front and

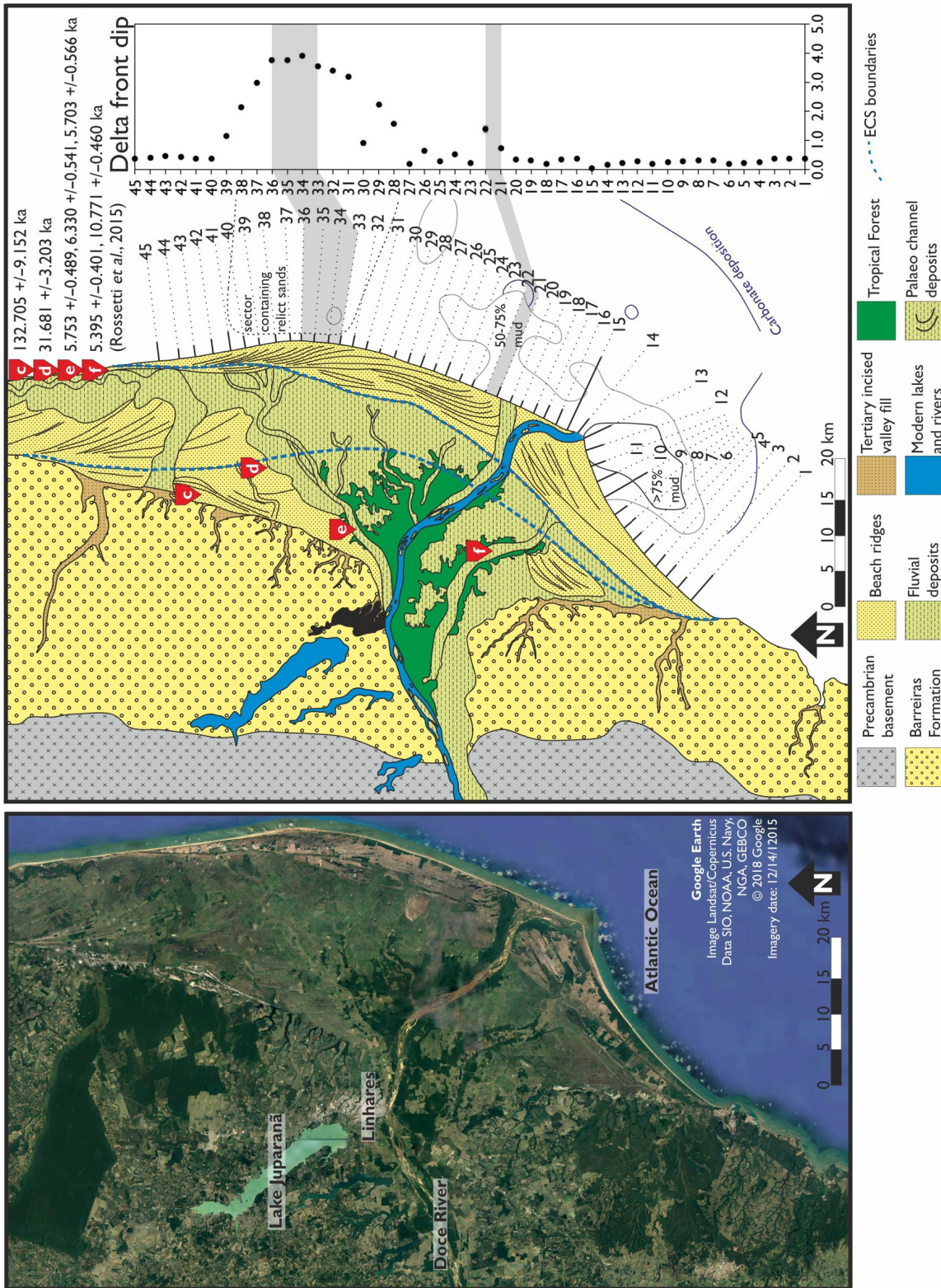


Fig. 5. Satellite view of the Doce delta (left) with interpreted features and cliniform dip transects (right, error bars in grey are based on the inferred resolution of the remote sensing data). The placement of the element complex set (ECS) boundaries is based on Ainsworth *et al.* (2019). The extent of the Barreiras Formation is taken from Dominguez *et al.* (1987).

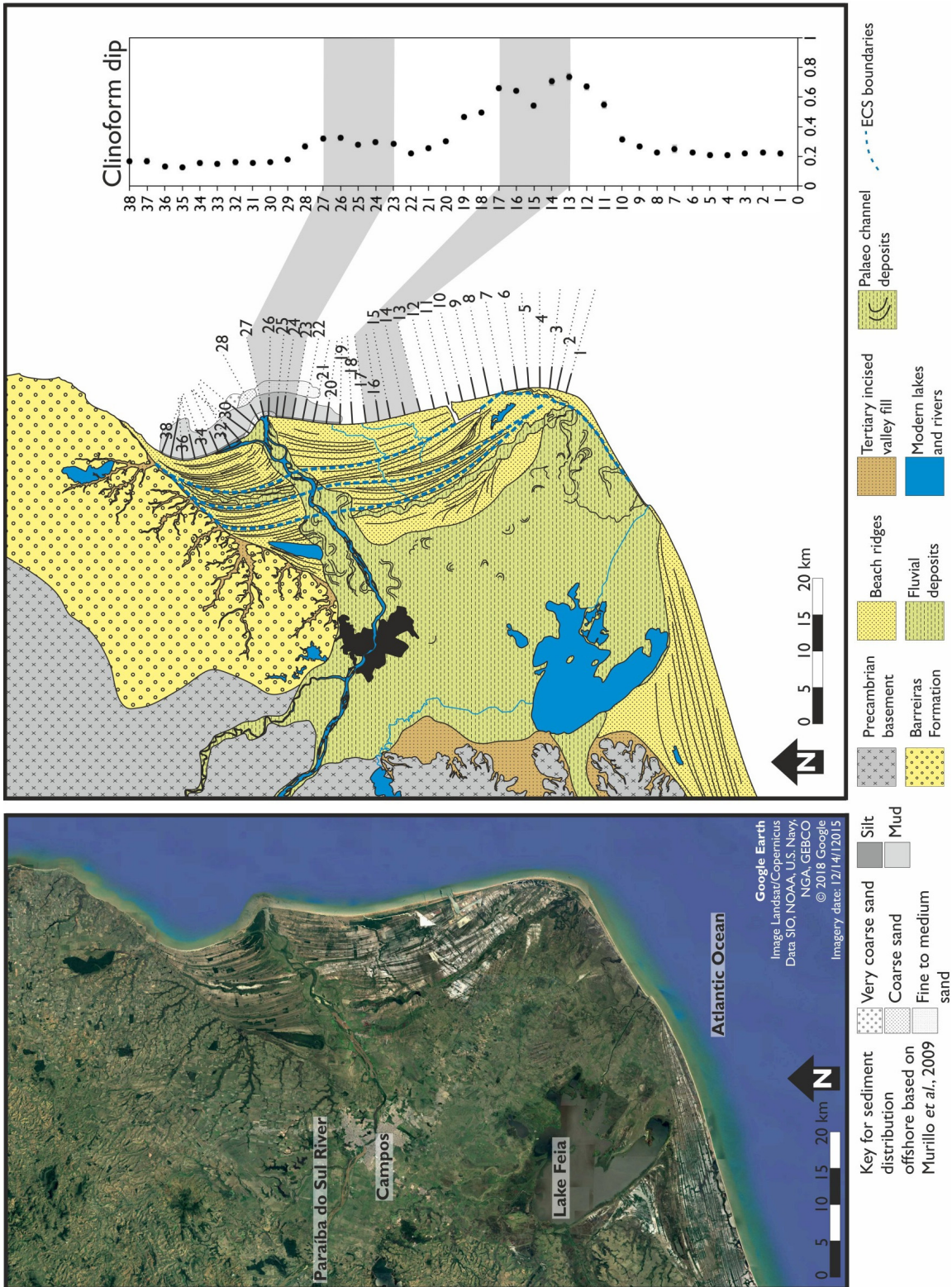


Fig. 6. Satellite view of the Paraíba do Sul delta (left, error bars in grey are based on the inferred resolution of the remote sensing data) with interpreted features and clinoform dip transects (right). The placement of the element complex set (ECS) boundaries is taken from Ainsworth *et al.* (2019). The extent of the Barreiras Formation is taken from Dominguez *et al.* (1987).

shallower dips of 0.12° in the central part (Fig. 3). However, there are two outliers from this trend in the central part where the dips reach up to 0.38° (Fig. 7). Delta front dip along strike of the Jequitinhonha River delta shows three high points (Fig. 4): one in the south with 0.25° ; one in the centre reaching 0.32° ;

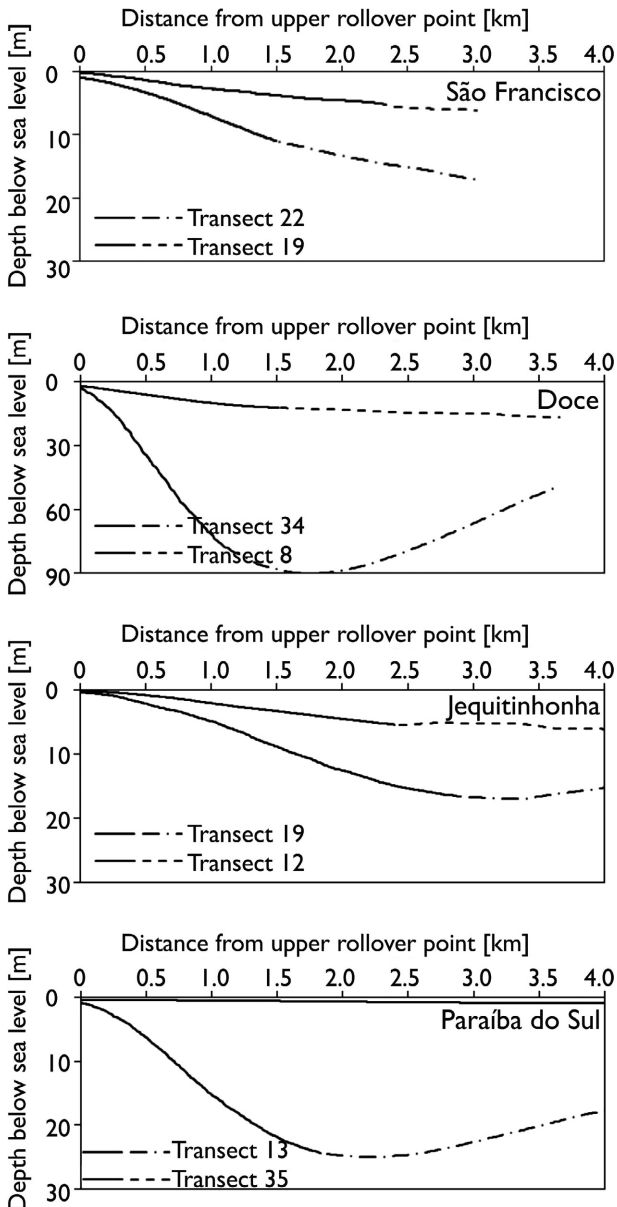


Fig. 7. Each figure shows the transect with the steepest and the transect with the lowest delta front dip for the four south-east Brazilian deltas. The dip sections are based on bathymetry profiles from Google Earth© which carry a horizontal and vertical error of approximately 10 m and 1 m, respectively (see *Methodology* section). Note the change in depth-scale for the Doce delta diagram.

and one in the north going up to 0.36° . In between those high points, dips are between 0.13° and 0.22° . The two northernmost points measured along strike also show higher dips of 0.29° and 0.37° . The Doce River has the steepest delta front dip of all deltas and the overall dip distribution has two very distinct areas of steep dip in the centre reaching up to 3.91° in the centre-north and 1.39° centre-south position (Figs 5 and 7). The rest of the along strike profile of the Doce delta shows values between 0.03° and 0.71° . In a similar manner to the Doce River delta, the Paraíba do Sul delta has two areas of high delta front dip in its centre and lower dip along the rest of the delta front (between 0.12° and 0.25° , Figs 6 and 7). The steeper dips are found in the centre-south position reaching 0.74° with the steepest dip in the centre-north position only reaching 0.32° . Both areas of steep dip of the Paraíba do Sul delta appear two-pronged with the bathymetry profile showing two shoulders of high delta front dip values with a small decrease in dip in between them.

HALIBUT DELTA, OUTER MORAY FIRTH, NORTH SEA

Study area and geological history

The Eocene Halibut Delta lies in the Outer Moray Firth east of the Scottish mainland (Fig. 8). It was documented and described in detail by Zimmer *et al.* (2019). The delta was deposited north of the Halibut Horst on the North Halibut Shelf. The North Sea Basin is a tripartite system with the Viking Graben to the north, the Central Graben to the south and the Moray Firth to the west. The North Sea Basin underwent multiple phases of rifting starting with the establishment of a north-south trending graben system following the collapse of the Middle Jurassic thermal dome (Ziegler, 1990; Underhill & Partington, 1993; Quirie *et al.*, 2019). A later change in tectonic regime formed the WNW-ESE oriented horst and graben structures of the Moray Firth (Boldy & Brealey, 1990). Rifting lasted until the Lower Cretaceous and was followed by thermal subsidence of the North Sea Basin. During the Palaeocene, magmatic under-plating resulted in uplift in the area of the East Shetland Platform and the Scottish mainland in conjunction with the opening of the Atlantic Ocean (Stucky de

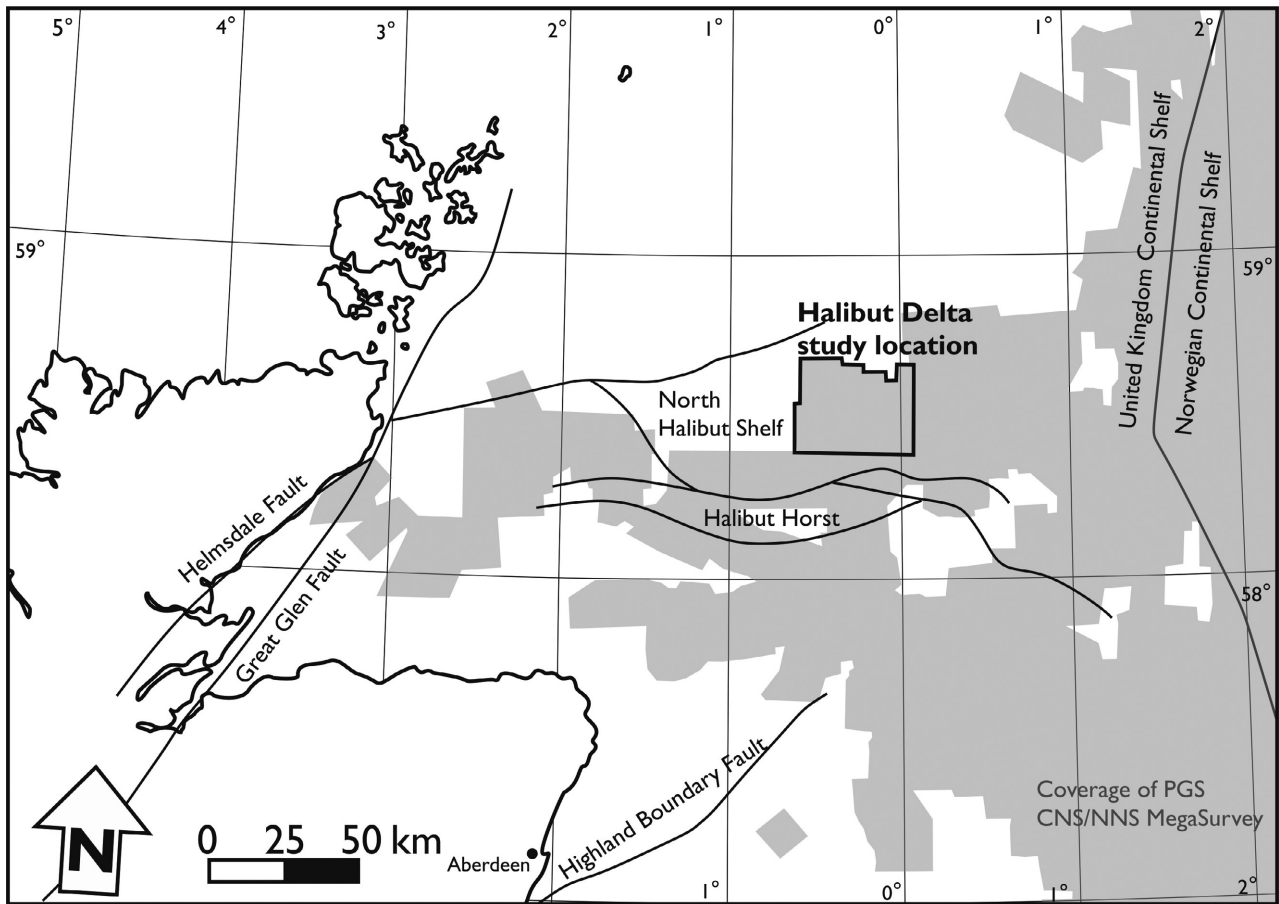


Fig. 8. Case study area of the Eocene Halibut Delta in the Outer Moray Firth showing a palaeogeographic interpretation based on RMS amplitude reflections (modified from Zimmer *et al.*, 2019). The black outline labelled Halibut Delta shows the location of Fig. 9.

Quay *et al.*, 2017; Hardman *et al.*, 2018). At the same time, global sea level displays a long-term eustatic fall from the Cretaceous onward (Haq *et al.*, 1988; Miller *et al.*, 2005). Local uplift coupled with global sea-level fall led to significantly increased sedimentation in the North Sea Basin from the north-west, forming deltaic successions such as the Upper Palaeocene–Lower Eocene Dornoch Formation which is characterized by thick deltaic sequences deposited in the Outer Moray Firth as well as along the eastern edge of the East Shetland Platform (Deegan & Scull, 1977; Mudge & Copestake, 1992; Underhill, 2001; Anell *et al.*, 2012). The deposition of the Dornoch Formation was followed by a relative sea-level lowstand in the area (Thomas & Hartley, 2014) during which coal seams and lowstand shoreface sands of the Balder Formation were deposited (Deegan & Scull, 1977; Mudge &

Copestake, 1992). The study area along with parts of the East Shetland platform were resubmerged during the basal Eocene transgression between 54 Ma and 52 Ma (Ypresian, Mudge, 2015). During the following regression, the deltaic succession studied here was deposited. Sedimentation during the start of the Eocene was more localized than during deposition of the Dornoch Formation (Underhill, 2001). The deltaic succession is characterized by fine to coarse-grained glauconitic sand which passes basinward into marine shales of the Horda Formation (Knox & Holloway, 1992). The Oligocene to Pliocene marine shale and clay deposits of the Westray and Nordland groups overlie the delta (Deegan & Scull, 1977; Knox & Holloway, 1992). These deposits are cross-cut by tunnel valleys which developed at the ice-sheet margins during Pleistocene glaciations (Wingfield, 1990; Rea *et al.*, 2018).

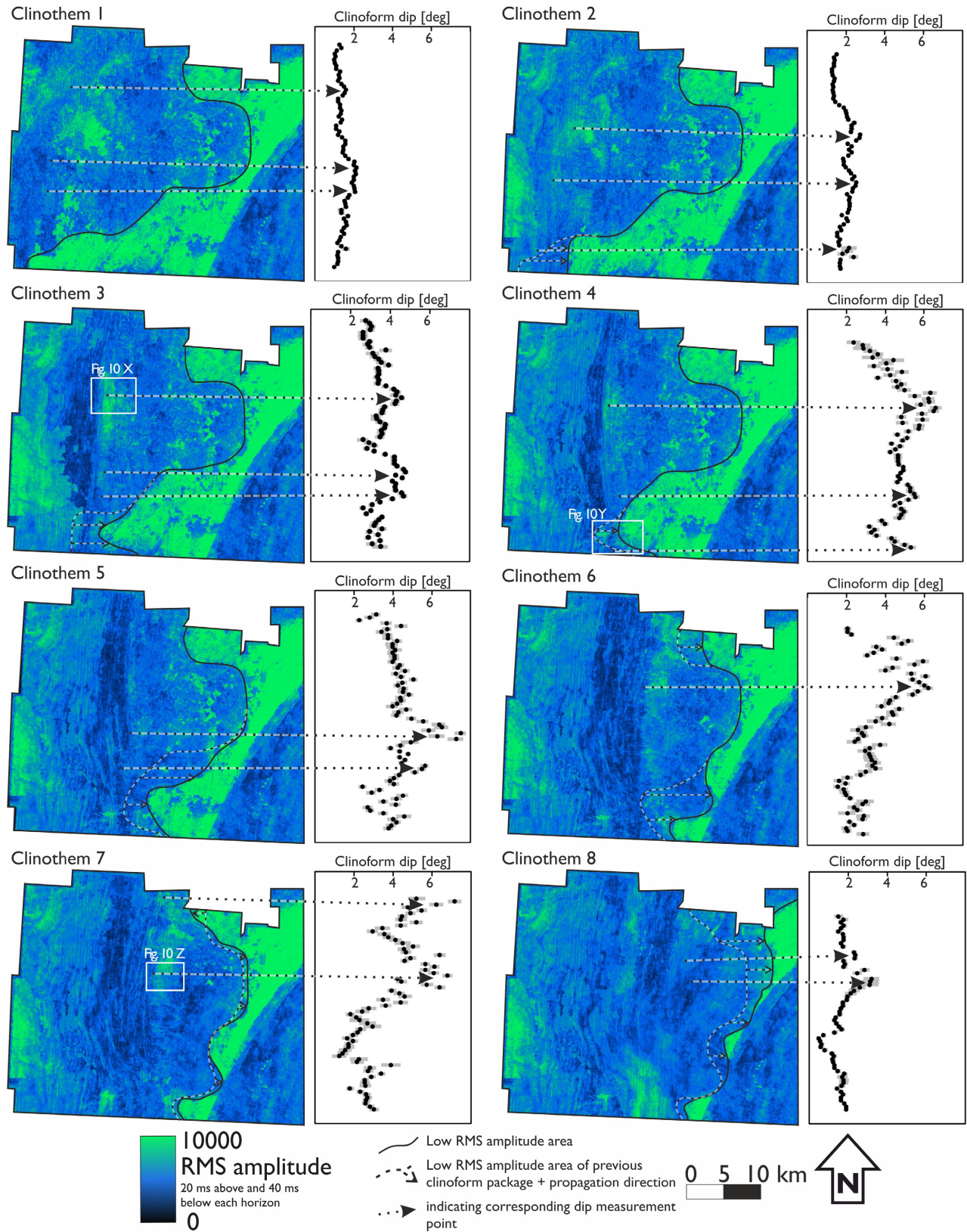


Fig. 9. Root mean square (RMS) amplitude maps of each individual clinothem shown with the cliniform dip measurements along strike. The error bars shown in grey are based on the horizontal and vertical resolution of the seismic data. The crescent shape in the east of the study area is an impression of the coastlines during deposition of the Balder Formation. For a detailed view of rectangles X, Y, and Z see Fig. 10.

Methodology

Measuring clinoform dip in 3D seismic

The 3D seismic dataset utilized in this study is the PGS CNS/NNS MegaSurvey, which covers large parts of the North Sea Basin including the British, Dutch, German, Danish and Norwegian continental shelf areas from 62°29'8"N to 54°08'18"N and from 4°35'29"W to 7°52'10"E (>148 000 km²). This regional 3D seismic dataset is made up of a merge of numerous datasets acquired throughout the North Sea Basin exploration history. The zero-phase normal polarity survey was available to a depth of 1 second two-way-time (TWT). The bin size is 50 m and the survey has a vertical sample interval of 4 ms. A vertical resolution of 13 m has been calculated based on a borehole-derived mean sediment velocity of 2050 m/s and a dominant frequency of 40 Hz at the examined depth. While for the south-east Brazilian deltas delta front dip has been measured along the current coastline, clinoform dip for the Halibut Delta was measured with reference to palaeo-shoreline strike interpreted for eight successive clinoform surfaces throughout the delta's development history (Figs 2 and 9). Clinoform dip was measured along multiple transects perpendicular to the palaeo-shoreline with a spacing of 405 m.

Time depth conversion, decompaction and attribute analysis

In the Halibut Delta study area checkshot data from eight wells were used for time depth conversion of the interpreted horizons upon which the clinoform dip measurements were based. Additionally, the pre-burial thickness of the deposits was determined to correct for the influence of compaction on the clinoform dip values (decompaction calculation after Allen & Allen, 2013). For decompaction purposes, the overlying sediment was treated as one layer of shaley sand using a surface porosity of 0.56 and a porosity coefficient of 0.39 (Sclater & Christie, 1980). Root mean square (RMS) amplitude was computed to image lithology on the clinoform surfaces of the individual clinoforms. The RMS amplitude attribute highlights horizontal changes in amplitude which are caused by the change in acoustic impedance between neighbouring lithologies. The RMS amplitude is frequently used to image lithology in shallow and deep marine settings (Posamentier & Kolla, 2003; Posamentier, 2004; Jackson *et al.*, 2010).

Halibut Delta clinoform dip along strike

Cli-noform dip for the Halibut Delta varies along strike for each clinothem interpreted in this study, showing up to three peaks in clinoform dip angle. Clinothems 1 to 4 show three peaks along strike (Fig. 9). All four clinothems have peaks in their clinoform dip in a similar central-southern and central-northern position, although each clinothem has one peak that deviates from this pattern. While high clinoform dips in clinothems 1 to 4 are generally more abundant towards the south, only clinothems 2 and 4 show a peak in clinoform dip angle in the far south of the study area. Clinothem 1 has a small peak of 1.5° in the north and a two-pronged peak further towards the south reaching 2.1°. The baseline in between those peaks for clinothem 1 remains at around 1.0°. In clinothem 2 two of the peaks are more centrally located (2.7° and 2.5°) with one smaller peak (1.8°) located further south. Clinothem 3 has two peaks in a central southern position which both measure a maximum of 4.7° and a slightly smaller peak further north reaching 4.6°. Clinothem 4 again shows three peaks which are more spread out than in clinothem 3. The highest clinoform dip (6.5°) for this clinothem is in a central northern position whereas the peaks in the south reach maximum clinoform dips of 5.6° and 5.3°. In clinothems 5 and 7 the number of peaks in clinoform dip reduces to two whereas clinothems 6 and 8 only show one peak. Overall, highest clinoform dips for these clinothems are present towards the north. In clinothem 5 the peaks are in a central position and reach 7.5° in the north and 5.6° in the south. The highest peak along strike of clinothem 6 lies in the north and reaches up to 6.2°. Clinothem 7 has a peak reaching 7.2° in a northern position and a smaller peak towards the centre (6.8°). Clinothem 8 only shows one significant peak in clinoform dip along strike towards the north which reaches 3.1°.

Attribute analysis of the Halibut Delta

With the seismic data it is possible to examine RMS amplitudes and other attributes. In Fig. 9 low RMS amplitudes (dark blue) mark the sandy main body of the clinothems. Palaeo-channel incisions on the clinothem surfaces are relatively faint on RMS amplitude maps (Figs 9 and 10). Faint incisions are visible as low RMS amplitude bands at the delta front (Fig. 10)

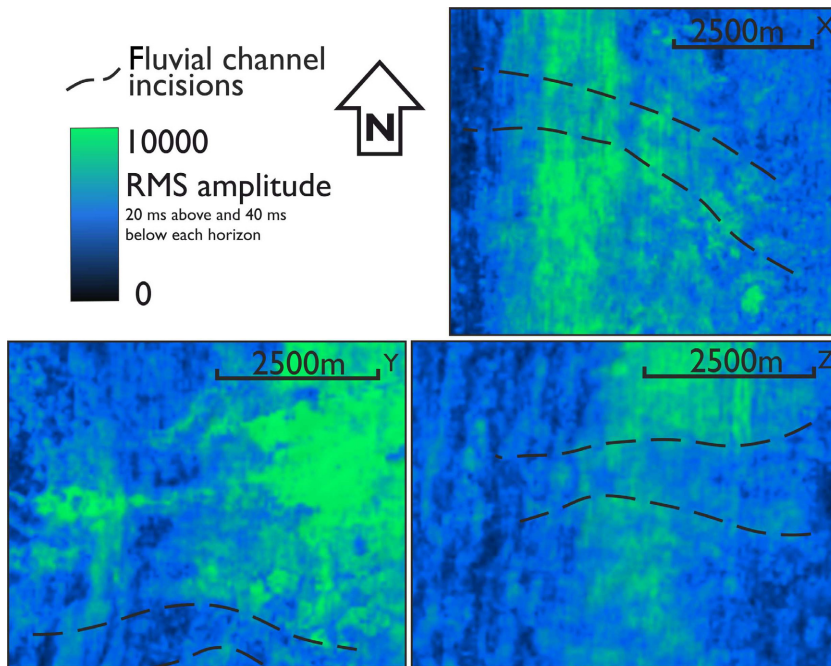


Fig. 10. Magnified view of faint channel incisions on the delta front of clinothem 3 (X), 4 (Y) and 7 (Z). For a larger map see Fig. 9.

which could be associated with mass transport deposits originating at the location of the fluvial input points and transporting sediment down the delta front towards the offshore transition zone. The RMS maps also show two broad, lobate tongues of low amplitudes in front of the delta which extend eastward replacing the otherwise high amplitudes there. In the south, the low amplitude tongue begins with clinothem 2 whereas in the northern part, the low amplitude tongue is only present from clinothem 6 onward. These low amplitude areas extend a short distance beyond the Balder Formation palaeo-coastline and are in line with the location of highest clinoform dips along strike for most of the clinothem.

Palaeo-channel incisions on the delta plain of the Halibut Delta are faint at best. There are multiple reasons for this to be the case. Firstly, from clinothem 1 to 6 normal regression followed by forced regression took place during which sediment was scavenged from each preceding clinothem. Clinothem 7 and 8 are transgressive deposits which in turn eroded and redeposited sediment from the underlying regressive systems tract. Secondly, the sediments infilling the closely overlying glacial tunnel valleys typically have very strong reflections. This influences the spectral decomposition maps through their broad frequency content and results in a bright response, masking subtle variations on the delta top itself. In addition to that, the change in

lithology between channel deposit and clinothem might not be pronounced enough to produce a sufficient change in amplitude or frequency to be visible on an attribute map.

SYNTHESIS OF RESULTS

Delta front dip is a modern proxy for clinoform dip and provides an opportunity to compare modern and ancient systems. According to Ainsworth *et al.* (2019), a delta body is classified as an element-complex assemblage which is made up of multiple element-complex sets representing individual delta lobes. The delta front dip measurements presented here for the south-east Brazilian deltas are taken at the delta front of the element-complex assemblage. The variations measured in delta front dip are therefore a composite expression of multiple delta lobe and mouth bar deposits (element-complex sets). In contrast to that, the clinothem in the Halibut Delta represent beach-ridge sets which are classified as element-set pairs, a constituent of an element-complex set (Ainsworth *et al.*, 2019). Although clinoform dip and delta front dip are not measured on deposits of the same hierarchy in this classification scheme the results of both study areas are compared here. The discrepancy in scale must be considered as a measure of uncertainty that is a feature inherent to the data types used in this study.

It is apparent from both datasets that dip angles are highest near fluvial input points. In order to allow a more systematic comparison, the results for each system were normalized such that the dip value at the inferred fluvial input point (marked by an arrow in Fig. 9 and by grey bars in Figs 3 to 6) was set to '1' and the clinoform dip values away from it were calculated as fractions of the maximum dip. The data were plotted with normalized clinoform dip against distance from fluvial input point for two distance brackets (Figs 11 and 12). From the location of the fluvial input point to a distance of 10 km away, clinoform dip decreases. A trendline was added to the data which shows a reasonable coefficient of determination (R^2 of 0.5). At 7.2 km away from the fluvial input point, clinoform dip halves on this trend line (marked by blue 'X' in Figs 11 and 12). The trendlines for the individual deltas vary between a high coefficient of determination of 0.7 for the Paraíba do Sul delta and Halibut Delta clinothems 7 and 8 and a low coefficient of determination of 0.3 for the São Francisco Delta and Halibut Delta clinothem 5 (Table 2). The coefficient of determination for individual trendlines

is generally higher for the Halibut Delta clinothems. From 10 to 20 km away from the fluvial input point clinoform dip does not show a trend but most points lie close to or below half the maximum clinoform dip (normalized dip of 0.5). It should be noted that the deflection of the river mouth and its associated sediment accumulation by longshore currents is challenging to reconstruct for systems in the subsurface and introduces a measure of uncertainty into the inferred location of palaeo-river mouths, especially in the examined Halibut Delta dataset.

DISCUSSION

High delta front dip and coarser sediment correlate with proximity to fluvial input points (Fig. 11). These include both modern and recent channels in the south-east Brazilian examples, suggesting that dip angles may persist after avulsion of delta channels. Palaeo-channels of the Doce delta are visible on the delta top and a palaeo-channel north of the modern Doce River course has been dated to between 6.3 (± 0.541) ka and 5.7 (± 0.566) ka (Rossetti *et al.*, 2015,

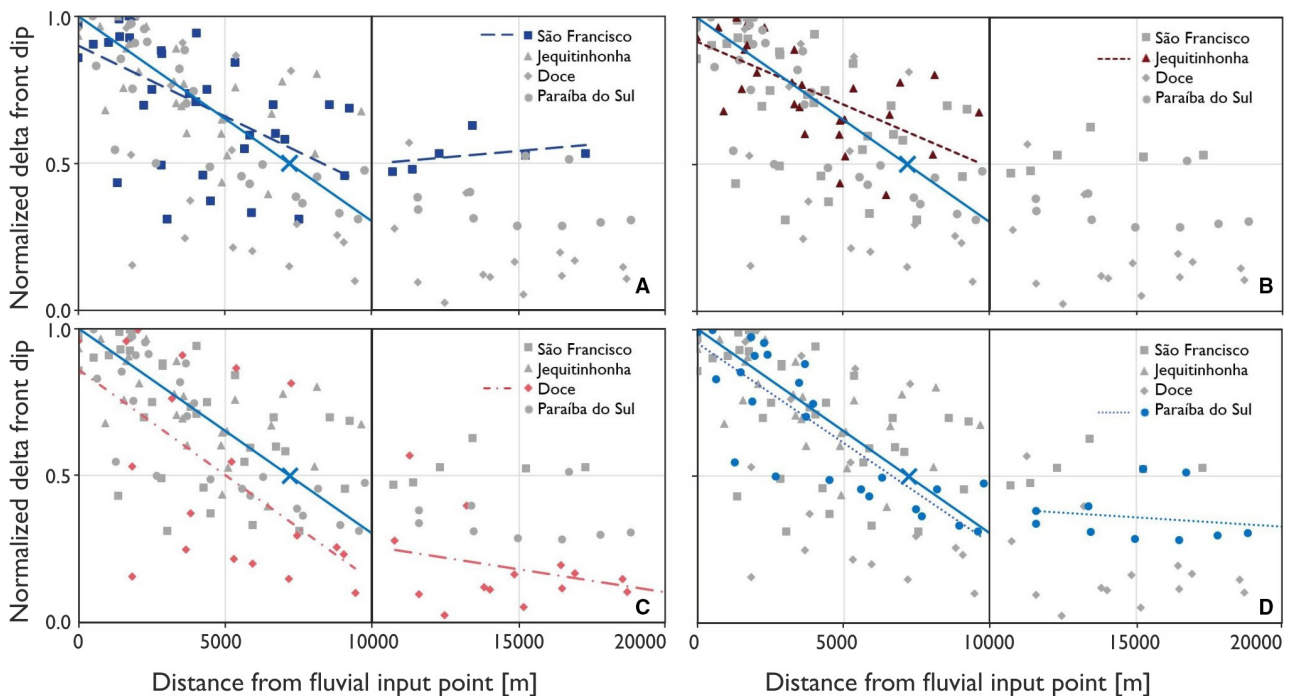


Fig. 11. Normalized delta front dip shown against distance from fluvial input point for the clinothems of the south-east Brazilian deltas (A: São Francisco, B: Jequitinhonha, C: Doce, D: Paraíba do Sul). The trendlines are computed for the distance bands of 0 to 10 km and 10 to 20 km separately. Please refer to Figs 3 to 6 for error bars based on the horizontal and vertical resolution of the data.

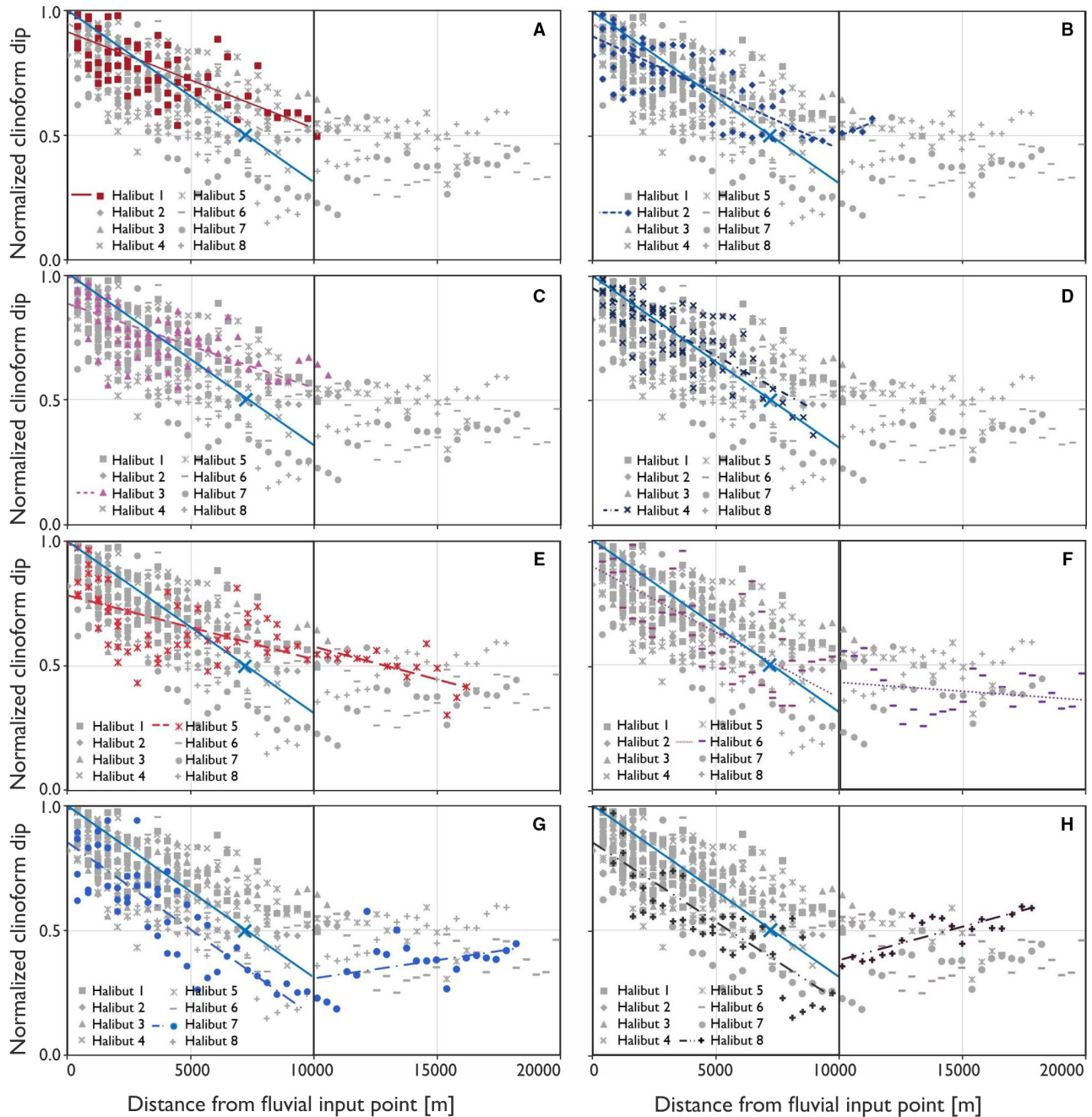


Fig. 12. Normalized clinof orm dip shown against distance from fluvial input point for the clinothems of the Halibut Delta (A: Clinothem 1, B: Clinothem 2, C: Clinothem 3, D: Clinothem 4, E: Clinothem 5, F: Clinothem 6, G: Clinothem 7, H: Clinothem 8). The trendlines are computed for the distance bands of 0 to 10 km and 10 to 20 km separately. Please refer to Fig. 9 for error bars based on the horizontal and vertical resolution of the data.

marker 'c' in Fig. 5). The location of this channel's palaeo-river mouth aligns with high delta front dips at transects 33 to 36 measured in this study. Sediment grab samples from this area record coarse sediment which is partly cemented and has been interpreted to have been deposited by an ancient riverine input point

(Quaresma *et al.*, 2015). A second palaeo-channel which skirts the current Doce River channel and has its palaeo-river mouth just north of the current river mouth (marker 'e' in Fig. 5) also lines up with a peak in delta front dip, albeit a smaller one. The current river mouth does not coincide with a significant change in delta front

Table 2. R^2 values for clinoform dip and delta front dip against distance from fluvial input point.

CLINOTHEM	R^2 in distance bands from fluvial input point 0–10 km	R^2 in distance bands from fluvial input point 10–20 km	DELTA	R^2 in distance from fluvial input point 0–10 km	R^2 in distance from fluvial input point 10–20 km
Halibut 1	0.51	n.a.	São Francisco	0.34	0.15
Halibut 2	0.64	0.58	Jequitinhonha	0.43	n.a.
Halibut 3	0.48	n.a.	Doce	0.38	0.11
Halibut 4	0.65	n.a.	Paraíba do Sul	0.73	0.04
Halibut 5	0.28	0.46			
Halibut 6	0.58	0.06			
Halibut 7	0.74	0.16			
Halibut 8	0.72	0.68			

n.a. = not available due to missing data in the 10 to 20 km distance bands.

dip which suggests that the systems take time to adjust and develop a steeper delta front. Sediment grab samples from the delta front of the Doce River record 75% mud south of the river mouth (Quaresma *et al.*, 2015) which is in accordance with the low delta front dips recorded in this study. It is worth noting that the delta front dips measured for the Doce River delta are an order of magnitude higher than the delta front dips of the other deltas examined here. Drainage area and shelf width are unlikely to be the source of this difference since these are comparable with the other examined deltas (Table 1). The lower inflection point of the steepest delta front dip profile of the Doce delta is recorded at close to 90 m below sea level (Fig. 7). For the other three deltas, the lower inflection point of the steepest delta front dip profile lies in much shallower water depth (between 10 m and 25 m, Fig. 7). This difference in water depth provides increased accommodation for the Doce delta and could cause the higher delta front dips.

Sediment samples seaward of the current mouth of the Paraíba do Sul River record coarse sediment at the immediate coastline as well as a tongue of coarse-grained and fine to medium-grained sand deposited 2.5 km offshore of the river mouth (Murillo *et al.*, 2009). Coarse-grained sand in two locations in front of the current river mouth along with high delta front dips at the corresponding transects measured in this study suggests that the Paraíba do Sul has occupied its current channel position long enough to have deposited substantial amounts of sediment. However, 15 km south of the current river mouth delta front dip reaches its highest values along strike for the Paraíba do Sul delta. No palaeo-channels are apparent on the delta top in

this location and there are no sediment grab samples documented far enough south to identify the lithology offshore. It is likely that the Paraíba do Sul occupied a channel halfway between the SSE directed palaeo-channel active during the Pleistocene (Martin *et al.*, 1985; Martin *et al.*, 1993) and the currently active channel position for a substantial amount of time to leave such a significant impact on delta front dip. The small streams traversing the beach ridges in the southern half of the delta plain could be exploiting a palaeo-channel course underlying the most recently deposited beach ridges. Although longshore currents are not uniform along the Paraíba do Sul delta front, higher delta front dips in the south could be due to northward directed longshore currents in this area, favouring deposition of coarser material.

Neither the São Francisco River nor the Jequitinhonha have been as extensively studied and the data on sediment distribution for these deltas are sparse. The São Francisco River has its highest delta front dip along strike at the position of the current river mouth (transects 21 and 22, Fig. 3). North, at Pontal de Peba, and in the south at the location of a small river (Papagaio River) delta front dip is higher again suggesting that rivers have been contributing sediment to the delta front at these locations in the past. Additionally, with longshore currents directed towards the south-west, the northern part of the São Francisco delta is subjected to greater wave influence, depositing coarser material than is found on the southern flank. This is reflected in the generally higher delta front dips in the north. The rivers to the north of the Jequitinhonha, the Pardo and Salsa rivers, correspond to a peak in delta front dip (transects 27 and 28,

Fig. 4) and given that they are said to have been larger rivers contributing to beach ridge formation during the Holocene (Dominguez *et al.*, 1987; Martin *et al.*, 1993) it is likely that this peak in delta front dip records the palaeo-river mouth location for one of these rivers.

Overall, the correlation between high delta front dip along strike, coarse sediment either at the delta front or in the offshore transition zone and the location of palaeochannels on the delta top support the interpretation that high delta front dips are found where the river mouth is located at present or has been located in the past. The influence of storm or flood events on grain-size distribution around the river mouth has not been investigated in this study but has been shown to result in significant changes in sediment distribution observable on short timescales (Zăinescu *et al.*, 2019). Remobilization of finer sediment during storm and flood events and redistribution along the delta front, through wave action and longshore currents, may lead to a higher concentration of coarse grain sizes at the river mouth. The coarse sediment allows for higher clinofrom dips which are in turn an indicator for the current river mouth or a palaeo-river mouth (Fig. 12).

Dip development with regard to the location of fluvial input points

To identify whether dip development along strike could be used for the prediction of the palaeo-river mouth location, dip measurements have been normalized and plotted in relation to their distance from the fluvial input point (Figs 11 and 12). Plotting this normalized dip data against the distance from the (inferred) fluvial input point shows that there is a steady decrease in delta front/clinofrom dip in the first 10 km either side of the fluvial input point with an average reduction in dip of 50% of its maximum value. This is the area where coarse and immature sediment from riverine input plays a significant role in the sediment budget of the delta front, causing high delta front/clinofrom dips. Lateral sediment dispersal does not seem to carry significant amounts of the coarser sediment further than 10 km away from the fluvial input point. It has been suggested that transport offshore is significant in river-dominated clinofroms which are found to be associated with deposition of coarse-grained sediment at the shoreface and with transport of the sediment to the offshore transition zone (Cosgrove *et al.*, 2018). Ten to 20 km away from the input point values are generally below 50% of the

maximum clinofrom dip but the data distribution is more chaotic and does not show a further decreasing trend. Sediment is reworked by longshore currents and wave action and overall clinofrom dips are lower in this area. The river-dominated character of the clinofrom is not prevalent any more at this distance from the fluvial input point, grain sizes are finer and shore-parallel sediment transport prevails over down-dip transport (Cosgrove *et al.*, 2018). The significant changes in clinofrom dip along strike illustrate that the processes which lead to sediment transport at the front of a wave-dominated delta are not uniform, and that close to the river mouth transport processes are river-dominated rather than wave-dominated. Given enough data points, dip variation along strike can thus be used as an indicator for the location of fluvial input points and it can be assumed that *ca* 10 km away from the fluvial input point wave-dominated processes are more influential than riverine input and sediment transport.

A larger drainage area does not seem to have a significant effect on delta front dip, with the São Francisco displaying similar dips to the Paraíba do Sul and Jequitinhonha delta fronts, despite its much larger drainage area. The south-east Brazilian deltas were also deposited in a passive margin, whereas deposition of the Halibut Delta took place towards the end of active rifting. Still, this difference in tectonic regime does not impede the comparison. However, the deltas examined here were chosen for their similarity and comparability. Marked differences in factors such as overall grain-size distribution, sediment supply and wave regime might prove to influence delta front dip distribution.

The results presented here have significant implications for predicting reservoir properties in more deeply buried, less well imaged delta systems, in the subsurface. Jackson *et al.* (2010) illustrated that, with amplitude analysis, distributary channels and beach ridge complexes could be imaged from the Brent Group reservoirs of the Oseberg Ost area of the Norwegian North Sea. Recent advances in seismic geomorphology and seismic attribute analysis (Posamentier *et al.*, 2007; Reijnenstein *et al.*, 2011; Patruno *et al.*, 2015b; Klausen *et al.*, 2016; He *et al.*, 2017) could improve on such mapping. Given the known position of input points and the relationships to grain size and clinofrom dip, this information could be used to condition the property modelling workflow when building reservoir models (Howell *et al.*, 2014).

CONCLUSION

The locations of deltaic river mouths can be inferred from the along strike development of clinoform dip. Clinoform dip is highest at the river mouth. Within the first 7.2 km away from it, maximum clinoform dip decreases by half. This has important implications for the facies and grain-size distribution of the associated clinothem. Coarse grain sizes are more abundant close to the river mouth, and fine sand, silt and clay are found further away from the fluvial input point. Further work should be carried out to verify the findings of this study by collecting and dating samples on the delta top and the delta front of the Jequitinhonha and São Francisco deltas which suffer from sparse data coverage. Additional targeted sampling of the better studied Doce and Paraíba do Sul deltas could be carried out guided by the findings from this work.

ACKNOWLEDGEMENTS

This work was undertaken as part of the SAFARI project in a collaboration between the University of Aberdeen, United Kingdom and NORCE in Bergen, Norway. SAFARI is sponsored by a consortium of oil companies, the Norwegian Petroleum Directorate, and the Norwegian Research Council. Details at www.safaridb.com. PGS generously provided the seismic data for this case study. Software used for seismic interpretation and satellite imagery analysis was Petrel 2016 by Schlumberger and Google Earth Pro 7.3.2.5491. We would like to thank the associate editor C. Fielding as well as the reviewers G. Hampson and E. Anthony for critically reviewing the manuscript and offering constructive advice leading to significant improvement of both text and figures.

DATA AVAILABILITY STATEMENT

The data that support the findings of this study are available from the corresponding author upon reasonable request.

REFERENCES

- Ainsworth, R.B., Vakarelov, B.K., Eide, C.H., Howell, J.A. and Bourget, J. (2019) Linking the High-Resolution Architecture of Modern and Ancient Wave-Dominated Deltas: Processes, Products, and Forcing Factors. *J. Sediment. Res.*, **89**, 168–185.
- Allen, P.A. and Allen, J.R. (2013) *Basin analysis: Principles and application to petroleum play assessment*. Wiley-Blackwell, Chichester, 633 pp.
- Amante, C.J. and Eakins, B.W. (2016) Accuracy of interpolated bathymetry in digital elevation models. *J. Coastal Res.*, **76**, 123–133.
- Andrade, A., Dominguez, J.M.L., Martin, L. and Bittencourt, A.C.S.P. (2003) Quaternary evolution of the Caravelas strandplain-southern Bahia State-Brazil. *Anais da Academia Brasileira de Ciências*, **75**, 357–382.
- Anell, I., Thybo, H. and Rasmussen, E. (2012) A synthesis of Cenozoic sedimentation in the North Sea. *Basin Res.*, **24**, 154–179.
- Anthony, E.J. (2015) Wave influence in the construction, shaping and destruction of river deltas: A review. *Mar. Geol.*, **361**, 53–78.
- Bastos, A.C. and Silva, C.G. (2003) Coastal morphodynamic and geomorphological compartments along the northeast littoral of Rio de Janeiro state, Brazil. *J. Coast. Res.*, **35**, 309–317.
- Bhattacharya, J.P. and Giosan, L. (2003) Wave-influenced deltas: Geomorphological implications for facies reconstruction. *Sedimentology*, **50**, 187–210.
- Bittencourt, A.C.d.S.P., Dominguez, J.M.L., Martin, L. and Silva, I.R. (2005) Longshore transport on the northeastern Brazilian coast and implications to the location of large scale accumulative and erosive zones: An overview. *Mar. Geol.*, **219**, 219–234.
- Boldy, S.A.R. and Brealey, S. (1990) Timing, nature and sedimentary result of Jurassic tectonism in the Outer Moray Firth. In: *Tectonic Events Responsible for Britain's Oil and Gas Reserves* (Eds Hardman, R.F.P. and Brooks, J.), pp. 259–279. Geological Society, London.
- Cartwright, J. and Huuse, M. (2005) 3D seismic technology: the geological "Hubble". *Basin Res.*, **17**, 1–20.
- Chang, H.K., Kowsmann, R.O., Figueiredo, A.M.F. and Bender, A.A. (1992) Tectonics and stratigraphy of the East Brazil Rift system: an overview. *Tectonophysics*, **213**, 97–138.
- Cohen, K.M., Finney, S.C., Gibbard, P.L. and Fan, J. (2013) The ICS international chronostratigraphic chart. *Episodes*, **36**, 199–204.
- Cosgrove, G.I.E., Hodgson, D.M., Poyatos-Moré, M., Mountney, N.P. and McCaffrey, W.D. (2018) Filter Or Conveyor? Establishing Relationships Between Clinoform Rollover Trajectory, Sedimentary Process Regime, and Grain Character Within Intraself Clinothem, Offshore New Jersey, USA. *J. Sediment Res.*, **88**, 917–941.
- Darros de Matos, R.M. (1999) History of the northeast Brazilian rift system: kinematic implications for the break-up between Brazil and West Africa. In: *The Oil and Gas Habitats of the South Atlantic* (Eds Cameron, N.R., Bate, R.H. and Clure, V.S.), pp. 55–73. Geological Society, London.
- Deegan, C.E. and Scull, B.J. (1977) A standard lithostratigraphic nomenclature for the Central and Northern North Sea. *Inst. Geol. Sci. Rep.*, **77**(25), 1–35.
- Dominguez, J.M.L. (1996) The São Francisco Strandplain: a Paradigm for Wave-Dominated Deltas? In: *Geology of Siliciclastic Shelf Seas*. (Eds De Batist, M. and Jacobs, P.), pp. 217–231. Geological Society, London.
- Dominguez, J.M.L. (2009) The coastal zone of Brazil. In: *Geology and Geomorphology of Holocene Coastal Barriers of Brazil* (Eds Dillenburg, S.R. and Hesp, P.A.), pp. 17–51. Springer, Berlin, Heidelberg.
- Dominguez, J.M.L., Martin, L. and Bittencourt, A.C.S.P. (1987) Sea-Level History and Quaternary Evolution of

- River Mouth-Associated Beachridge Plains Along the East-Southeast Brazilian Coast: A Summary. In: *Sea-Level Fluctuation and Coastal Evolution* (Eds Nummedal, D., Pilkey, O.H. and Howards, J.D.), pp. 115–127. SEPM Society for Sedimentary Geology, Tulsa.
- Evenstar, L., Sparks, R., Cooper, F. and Lawton, M.** (2018) Quaternary landscape evolution of the Helmand Basin, Afghanistan: Insights from staircase terraces, deltas, and paleoshorelines using high-resolution remote sensing analysis. *Geomorphology*, **311**, 37–50.
- Hampson, G.J., Morris, J.E. and Johnson, H.D.** (2015) Synthesis of time-stratigraphic relationships and their impact on hydrocarbon reservoir distribution and performance, Bridport Sand Formation, Wessex Basin, UK. In: *Strata and Time: Probing the Gaps in Our Understanding* (Eds Smith, D.G., Bailey, R.J., Burgess, P.M. and Fraser, A.J.), pp. 199–222. Geological Society, London.
- Haq, B.U., Hardenbol, J. and Vail, P.R.** (1988) Mesozoic and Cenozoic chronostratigraphy and cycles of sea-level change. In: *Sea level changes: an integrated approach* (Ed. Wilgus, C.K.), pp. 71–108. SEPM Society of Economic Paleontologists and Mineralogists, Tulsa.
- Hardman, J.P.A., Schofield, N., Jolley, D.W., Holford, S.P., Hartley, A.J., Morse, S., Underhill, J., Watson, D.A. and Zimmer, E.H.** (2018) Prolonged dynamic support from the Icelandic plume of the NE Atlantic margin. *J. Geol. Soc.*, **175**, 396–410.
- Hartley, A.J., Weissmann, G.S., Nichols, G.J. and Warwick, G.L.** (2010) Large distributive fluvial systems: characteristics, distribution, and controls on development. *J. Sediment. Res.*, **80**, 167–183.
- Hartley, A.J., Owen, A., Weissmann, G.S. and Scuderi, L.A.** (2018) Modern and Ancient Amalgamated Sandy Meander-Belt Deposits: Recognition and Controls on Development. In: *Fluvial Meanders and Their Sedimentary Products in the Rock Record* (Eds Ghinassi, M., Colombera, L., Mountney, N.P., Reesink, A.J.H. and Bateman, M.), pp. 349–383. International Association of Sedimentologists, Oxford.
- He, M., Zhuo, H., Chen, W., Wang, Y., Du, J., Liu, L., Wang, L. and Wan, H.** (2017) Sequence stratigraphy and depositional architecture of the Pearl River Delta system, northern South China Sea: An interactive response to sea level, tectonics and paleoceanography. *Mar. Pet. Geol.*, **84**, 76–101.
- Hein, C.J., Fitzgerald, D.M., Cleary, W.J., Albernaz, M.B., de Menezes, J.T. and Klein, A.H.** (2013) Evidence for a transgressive barrier within a regressive strandplain system: Implications for complex coastal response to environmental change. *Sedimentology*, **60**, 469–502.
- Helland-Hansen, W. and Martinsen, O.J.** (1996) Shoreline trajectories and sequences: description of variable depositional-dip scenarios. *J. Sediment Res.*, **66**, 670–688.
- Helland-Hansen, W. and Hampson, G.J.** (2009) Trajectory analysis: concepts and applications. *Basin Res.*, **21**, 454–483.
- Henriksen, S., Hampson, G.J., Helland-Hansen, W., Johannessen, E.P. and Steel, R.J.** (2009) Shelf edge and shoreline trajectories, a dynamic approach to stratigraphic analysis. *Basin Res.*, **21**, 445–453.
- Henriksen, S., Helland-Hansen, W. and Bullimore, S.** (2011) Relationships between shelf-edge trajectories and sediment dispersal along depositional dip and strike: a different approach to sequence stratigraphy. *Basin Res.*, **23**, 3–21.
- Howell, J.A., Martinius, A.W. and Good, T.R.** (2014) The application of outcrop analogues in geological modelling: a review, present status and future outlook. *Geol. Soc., London, Spec. Public.*, **387**, 1–25.
- Howell, J.A., Skorstad, A., MacDonald, A., Fordham, A., Flint, S., Fjellvoll, B. and Manzocchi, T.** (2008) Sedimentological parameterization of shallow-marine reservoirs. *Petrol. Geosci.*, **14**, 17–34.
- Jackson, C.A.L., Grunhagen, H., Howell, J.A., Larsen, A.L., Andersson, A., Boen, F. and Groth, A.** (2010) 3D seismic imaging of lower delta-plain beach ridges: lower Brent Group, northern North Sea. *J. Geol. Soc.*, **167**, 1225–1236.
- Johannessen, E.P. and Steel, R.J.** (2005) Shelf-margin clinofolds and prediction of deepwater sands. *Basin Res.*, **17**, 521–550.
- Kantorowicz, J., Bryant, I. and Dawans, J.** (1987) Controls on the geometry and distribution of carbonate cements in Jurassic sandstones: Bridport Sands, southern England and Viking Group, Troll Field, Norway. In: *Diagenesis of Sedimentary Sequences* (Ed. Marshall, J.D.), pp. 103–118. Geological Society, London.
- Klausen, T.G., Ryseth, A., Helland-Hansen, W. and Gjelberg, H.K.** (2016) Progradational and backstepping shoreface deposits in the Ladinian to Early Norian Snadd Formation of the Barents Sea. *Sedimentology*, **63**, 893–916.
- Knox, R.W.O.B. and Holloway, S.** (1992) Paleogene of the Central and Northern North Sea. In: *Lithostratigraphic nomenclature of the UK North Sea* (Eds Knox, R.W.O.B. and Holloway, S.), pp. 1–127. Keyworth, British Geological Survey.
- Lawver, L.A., Gahagan, L.M. and Coffin, M.F.** (1992) The development of paleoseaways around Antarctica. In: *The Antarctic Paleoenvironment: A Perspective on Global Change: Part One* (Eds Kennett, J.P. and Warkne, D.A.), pp. 7–30. American Geophysical Union, Washington, DC.
- Loseth, T.M. and Ryseth, A.** (2003) A depositional and sequence stratigraphic model for the Rannoch and Etive formations, Oseberg Field, northern North Sea. *Norw. J. Geol.*, **83**, 87–106.
- Macdonald, D., Gomez-Perez, I., Franzese, J., Spalletti, L., Lawver, L., Gahagan, L., Dalziel, I., Thomas, C., Trewin, N. and Hole, M.** (2003) Mesozoic break-up of SW Gondwana: implications for regional hydrocarbon potential of the southern South Atlantic. *Mar. Pet. Geol.*, **20**, 287–308.
- Martin, L. and Suguio, K.** (1992) Variation of coastal dynamics during the last 7000 years recorded in beach-ridge plains associated with river mouths: example from the central Brazilian coast. *Palaeogeogr. Palaeoclimatol. Palaeoecol.*, **99**, 119–140.
- Martin, L., Suguio, K. and Flexor, J.** (1993) As flutuações de nível do mar durante o quaternário superior e a evolução geológica de "deltas" brasileiros. *Boletim IG-USP. Publicação Espec.*, **15**, 1–186.
- Martin, L., Suguio, K., Flexor, J., Tessler, M. and Eichler, B.B.** (1985) Roundness in Holocene sands of the Paraíba do Sul coastal plain, Rio de Janeiro, Brazil. *J. Coastal Res.*, **1**, 343–351.
- Martin, L. and Dominguez, J.M.L.** (1994) Geological history of coastal lagoons. In: *Coastal Lagoon Processes* (Ed. Kjerfve, B.) *Elsevier Oceanography Series* edn, pp. 41–68. Elsevier, Amsterdam.

- Mayer, L., Jakobsson, M., Allen, G., Dorschel, B., Falconer, R., Ferrini, V., Lamarche, G., Snaith, H. and Weatherall, P. (2018) The Nippon Foundation—GEBCO seabed 2030 project: The quest to see the world's oceans completely mapped by 2030. *Geosciences*, **8**, 63.
- Milani, E.J., Rangel, H.D., Bueno, G.V., Stica, J.M., Winter, W.R., Caixeta, J.M. and Neto, O.P. (2007) Bacias sedimentares brasileiras: cartas estratigráficas. *Anexo ao Boletim de Geociências da Petrobrás*, **15**, 183–205.
- Miller, K.G., Kominz, M.A., Browning, J.V., Wright, J.D., Mountain, G.S., Katz, M.E., Sugarman, P.J., Cramer, B.S., Christie-Blick, N. and Pekar, S.F. (2005) The Phanerozoic record of global sea-level change. *Science*, **310**, 1293–1298.
- Mohriak, W., Nemčok, M. and Enciso, G. (2008) South Atlantic divergent margin evolution: rift-border uplift and salt tectonics in the basins of SE Brazil. In: *West Gondwana: Pre-Cenozoic Correlations Across the South Atlantic Region* (Eds Pankhurst, R.J., Trouw, R.A.J., de Brito Neves, B.B. and de Wit, M.J.), pp. 365–398. Geological Society, London.
- Mudge, D.C. and Copestake, P. (1992) Revised lower Palaeogene lithostratigraphy for the Outer Moray Firth, North Sea. *Mar. Pet. Geol.*, **9**, 53–69.
- Mudge, D.C. (2015) Regional controls on Lower Tertiary sandstone distribution in the North Sea and NE Atlantic margin basins. In: *Tertiary Deep-Marine Reservoirs of the North Sea Region* (Eds McKie, T., Rose, P.T.S., Hartley, A.J., Jones, D.W. and Armstrong, T.L.), pp. 17–42. Geological Society, London.
- Murillo, V.C., Silva, C.G. and Fernandez, G.B. (2009) Nearshore Sediments and Coastal Evolution of Paraíba do Sul River Delta, Rio de Janeiro, Brazil. *J. Coast. Res. Spec. Issue*, **56**, 650–654.
- Nicholls, R.J., Wong, P.P., Burkett, V.R., Codignotto, J., Hay, J., McLean, R., Ragoonaden, S. and Woodroffe, C.D. (2007) Coastal systems and low-lying areas. In: *Climate change 2007: impacts, adaptation and vulnerability. Contribution of Working Group II to the fourth assessment report of the Intergovernmental Panel on Climate Change* (Eds M.L. Parry, O.F. Canziani, J.P. Palutikof, P.J. van der Linden and C.E. Hanson), pp. 315–356. Cambridge University Press, Cambridge, UK.
- Nyberg, B. and Howell, J.A. (2016) Global distribution of modern shallow marine shorelines. Implications for exploration and reservoir analogue studies. *Mar. Pet. Geol.*, **71**, 83–104.
- Oliveira, E.N.d., Knoppers, B.A., Lorenzetti, J.A., Medeiros, P.R.P., Carneiro, M.E. and Souza, W.F.L.d. (2012) A satellite view of riverine turbidity plumes on the NE-E Brazilian coastal zone. *Brazil. J. Oceanogr.*, **60**, 283–298.
- Orton, G.J. and Reading, H.G. (1993) Variability of deltaic processes in terms of sediment supply, with particular emphasis on grain size. *Sedimentology*, **40**, 475–512.
- Patchineelam, S.R. and Smoak, J.M. (1999) Sediment accumulation rates along the inner eastern Brazilian continental shelf. *Geo-Mar. Lett.*, **19**, 196–201.
- Patruno, S., Hampson, G.J. and Jackson, C.A.L. (2015a) Quantitative characterisation of deltaic and subaqueous clinofolds. *Earth Sci. Rev.*, **142**, 79–119.
- Patruno, S., Hampson, G.J., Jackson, C.A.L. and Dreyer, T. (2015b) Clinofold geometry, geomorphology, facies character and stratigraphic architecture of a sand-rich subaqueous delta: Jurassic Sognefjord Formation, offshore Norway. *Sedimentology*, **62**, 350–388.
- Polizel, S.P. and Rossetti, D.D.F. (2014) Caracterização morfológica do delta do rio Doce (ES) com base em análise multissensor. *Revista Brasileira de Geomorfologia*, **15**, 311–326.
- Posamentier, H.W., Davies, R.J., Cartwright, J.A. and Wood, L. (2007) Seismic geomorphology—an overview. In: *Seismic Geomorphology: Applications to Hydrocarbon Exploration and Production* (Eds Davies, R.J., Posamentier, H.W., Wood, L.J. and Cartwright, J.A.), pp. 1–14. Geological Society, London.
- Posamentier, H.W. and Kolla, V. (2003) Seismic geomorphology and stratigraphy of depositional elements in deep-water settings. *J. Sediment. Res.*, **73**, 367–388.
- Posamentier, H.W. (2004) Seismic geomorphology: imaging elements of depositional systems from shelf to deep basin using 3D seismic data: implications for exploration and development. In: *3D Seismic Technology: Application to the Exploration of Sedimentary Basins* (Eds Davies, R.J., Cartwright, J.A., Stewart, S.A., Lappin, M. and Underhill, J.R.), pp. 11–24. Geological Society, London.
- Quaresma, V.d.S., Catabriga, G., Bourguignon, S.N., Godinho, E. and Bastos, A.C. (2015) Modern sedimentary processes along the Doce river adjacent continental shelf. *Brazilian Journal of Geology*, **45**, 635–644.
- Quirie, A.K., Schofield, N., Hartley, A., Hole, M.J., Archer, S.G., Underhill, J.R., Watson, D. and Holford, S.P. (2019) The Rattray Volcanics: Mid-Jurassic fissure volcanism in the UK Central North Sea. *J. Geol. Soc.*, **176**, 462–481.
- Rea, B.R., Newton, A.M., Lamb, R.M., Harding, R., Bigg, G.R., Rose, P., Spagnolo, M., Huuse, M., Cater, J.M. and Archer, S. (2018) Extensive marine-terminating ice sheets in Europe from 2.5 million years ago. *Science. Advances*, **4**(6), eaar8327.
- Reijnenstein, H.M., Posamentier, H.W. and Bhattacharya, J.P. (2011) Seismic geomorphology and high-resolution seismic stratigraphy of inner-shelf fluvial, estuarine, deltaic, and marine sequences, Gulf of Thailand. *AAPG Bulletin*, **95**, 1959–1990.
- Rich, J.L. (1951) Three critical environments of deposition, and criteria for recognition of rocks deposited in each of them. *Geol. Soc. Am. Bull.*, **62**, 1–20.
- Rocha, T.B.D., Fernandez, G.B. and de Oliveira Peixoto, M.N. (2013) Applications of ground-penetrating radar to investigate the Quaternary evolution of the south part of the Paraíba do Sul river delta (Rio de Janeiro, Brazil). *J. Coast. Res.*, **65**, 570–576.
- Rossetti, D.D.F., Polizel, S.P., Cohen, M.C.L. and Pessenda, L.C.R. (2015) Late Pleistocene-Holocene evolution of the Doce River delta, southeastern Brazil: implications for the understanding of wave-influenced deltas. *Mar. Geol.*, **367**, 171–190.
- Rossetti, D.F. and Góes, A.M. (2009) Marine influence in the Barreiras Formation, state of Alagoas, northeastern Brazil. *Anais da Academia Brasileira de Ciências*, **81**, 741–755.
- Santos, M.G., Hartley, A.J., Mountney, N.P., Peakall, J., Owen, A., Merino, E.R. and Assine, M.L. (2019) Meandering rivers in modern desert basins: Implications for channel planform controls and prevegetation rivers. *Sed. Geol.*, **385**, 1–14.
- Schwaborn, G., Dix, J., Bull, J. and Rachold, V. (2002) High-resolution seismic and ground penetrating radar-geophysical profiling of a thermokarst lake in the western Lena Delta, Northern Siberia. *Permafrost Periglacial Process*, **13**, 259–269.
- Slater, J.G. and Christie, P.A.F. (1980) Continental stretching: An explanation of the post-Mid-Cretaceous subsidence of the central North Sea Basin. *J. Geophys. Res. Solid Earth*, **85**, 3711–3739.

- Small, C.** and **Nicholls, R.J.** (2003) A global analysis of human settlement in coastal zones. *J. Coastal Res.*, **19**, 584–599.
- Souza, W.F.L.** and **Knoppers, B.** (2011) Fluxos de água e sedimentos a costa leste do Brasil: relações entre a tipologia e as pressões antrópicas. *Geochimica Brasiliensis*, **17**, 57–74.
- Stucky de Quay, G., Roberts, G.G., Watson, J.S.** and **Jackson, C.A.L.** (2017) Incipient mantle plume evolution: Constraints from ancient landscapes buried beneath the North Sea. *Geochem. Geophys. Geosyst.*, **18**, 973–993.
- Thomas, R.** and **Hartley, A.J.** (2014) Seismic geomorphology and sequence stratigraphy as tools for the prediction of reservoir facies distribution: an example from the Paleocene and earliest Eocene of the South Buchan Graben, Outer Moray Firth Basin, UKCS. In: *Tertiary Deep-Marine Reservoirs of the North Sea Region* (Eds McKie, T., Rose, P.T.S., Hartley, A.J., Jones, D.W. and Armstrong, T.L.), pp. 99–132. Geological Society, London.
- Underhill, J.R.** and **Partington, M.A.** (1993) Jurassic thermal doming and deflation in the North Sea: implications of the sequence stratigraphic evidence. *Geol. Soc., London, Petrol. Geol. Conf. series*, **4**(1), 337–345.
- Underhill, J.** (2001) Controls on the genesis and prospectivity of Paleogene palaeogeomorphic traps, East Shetland Platform, UK North Sea. *Mar. Pet. Geol.*, **18**, 259–281.
- Vail, P.R., Mitchum, R.M.** and **Thompson, S.** (1977) Seismic stratigraphy and global changes of sea level: Part 3. Relative changes of sea level from Coastal Onlap: section 2. Application of seismic reflection Configuration to Stratigraphic Interpretation. In: *Seismic Stratigraphy-Applications to Hydrocarbon Exploration* (Eds Payton, C.E.), pp. 63–81. American Association of Petroleum Geologists, Tulsa.
- Vilas Boas, G.S., Sampaio, F.J.** and **Pereira, A.** (2001) The Barreiras Group in the Northeastern coast of the State of Bahia, Brazil: depositional mechanisms and processes. *Anais da Academia Brasileira de Ciências*, **73**, 417–427.
- Weatherall, P., Marks, K.M., Jakobsson, M., Schmitt, T., Tani, S., Arndt, J.E., Rovere, M., Chayes, D., Ferrini, V.** and **Wigley, R.** (2015) A new digital bathymetric model of the world's oceans. *Earth Space Sci.*, **2**, 331–345.
- Wingfield, R.** (1990) The origin of major incisions within the Pleistocene deposits of the North Sea. *Mar. Geol.*, **91**, 31–52.
- Zăinescu, F., Vespremeanu-Stroe, A., Anthony, E., Tătu, F., Preoteasa, L.** and **Mateescu, R.** (2019) Flood deposition and storm removal of sediments in front of a deltaic wave-influenced river mouth. *Mar. Geol.*, **417**, 106015.
- Ziegler, P.A.** (1990) *Geological Atlas of Western and Central Europe*. Geological Society Publishing House, Bath, 332 pp.
- Zimmer, E., Howell, J., Schofield, N.** and **Gawthorpe, R.** (2019) Seismic geomorphology linked to sequence stratigraphy of an Eocene delta in the Outer Moray Firth, UKCS. *Mar. Pet. Geol.*, **104**, 150–167.

Manuscript received 19 April 2020; revision accepted 1 September 2020